Application of a Multicomponent Thermodynamic Model to Activities and Thermal Properties of 0–40 mol kg^{-1} Aqueous Sulfuric Acid from <200 to 328 K

Simon L. Clegg* and Peter Brimblecombe

School of Environmental Sciences, University of East Anglia, Norwich NR4 7TJ, U.K.

A multicomponent mole-fraction-based thermodynamic model has been fitted to osmotic coefficients, electromotive force measurements, degrees of dissociation of the HSO_4^- ion, differential heats of dilution, heat capacities, freezing points, and tabulated partial molal enthalpies of water for aqueous H_2SO_4, from <200 to 328 K and from 0 to 40 mol kg^{-1} at 1 atm pressure (1 atm = 101.325 kPa). The solution is treated as the mixture H^+–HSO_4^-–SO_4^{2-}–H_2O. The equations yield a self-consistent representation of activities, speciation, and thermal properties which, for practical applications, is readily extended to more complex mixtures. Activity products of solutions saturated with respect to solid phases $H_2SO_4 \cdot nH_2O$ (where n is 1, 2, 3, 4, or 6.5) are determined as functions of temperature. Thermodynamic properties and speciation are tabulated at 253.15, 273.15, 298.15, and 323.15 K.

1. Introduction

Aqueous sulfuric acid is important to industry, and its thermodynamic properties have been studied extensively over many years (*1*). Recent evaluations include those by Staples (*2*) and Rard *et al.* (*3*) (osmotic and activity coefficients at 298.15 K), Bolsaitis and Elliott (*4*) (vapor pressures), Zeleznik (*5*) (properties of aqueous and solid phases, excluding vapor pressures) and Clegg *et al.* (*6*) (osmotic and activity coefficients and thermal properties).

In the field of natural water chemistry, the thermodynamics of aqueous H_2SO_4 and of mixtures including H_2SO_4 are important for models of the evolution of urban aerosols (*7*), and predictions of the water content of acid ammonium sulfate aerosols in the troposphere (*8, 9*) and their equilibrium with atmospheric NH_3. The global stratospheric aerosol is composed largely of aqueous H_2SO_4, and the solubilities of, for example, HCl and HNO_3 (*10, 11*) are significant in determining the stratospheric response to injections of volcanic material, and especially the generation of active chlorine (during the polar winter) which leads to ozone depletion (*12*).

For such practical applications a treatment of the thermodynamic properties of aqueous H_2SO_4 that readily generalizes to solution mixtures is first required. This must extend to high concentration (~80 wt % for atmospheric studies), and to very low temperature, as values of about 190 K are reached in the polar stratosphere. The mole-fraction-based ion-interaction model of Pitzer, Simonson, and Clegg (*13, 14*) has been developed with such systems in mind, and is expressed in a general form for an indefinite number of ionic and neutral components over the entire range of mole fraction.

Recently, Clegg *et al.* (*6*) have utilized an extended form of the molality-based Pitzer ion-interaction model to represent activities and thermal properties of aqueous H_2SO_4 from 0 to 6 mol kg^{-1} and from 273.15 to 328.15 K. The equations, which represent the data almost to within experimental error, form the basis of an improved model for solution mixtures at moderate temperature and concentration and also define a number of thermodynamic parameters for the present study. Here we apply the mole-fraction-based model to a larger range of data, including osmotic coefficients, vapor pressures, electromotive forces (emfs), enthalpies, heat capacities, freezing temperatures, and solid phase ($H_2SO_4 \cdot 4H_2O$) equilibrium data from <200 to 328 K and from 0 to 40 mol kg^{-1} acid. The resulting equations, and associated parameters, can be used to calculate a self-consistent set of thermodynamic properties of aqueous H_2SO_4. They also form the basis of an extended model for aqueous mixtures containing H_2SO_4.

2. Model

The mole fraction model is based upon an expression for the excess Gibbs energy of the solution, consisting of an extended Debye–Hückel function and a Margules expansion in terms of the mole fractions of the solution components (*14*). Mole fractions are calculated on the basis of the individual ionic and molecular species present; thus, the mole fraction x_j of species j is given by

$$x_j = n_j / \sum_i n_i \qquad (1)$$

where n_i is the number of moles of species i, with cations, anions, and the solvent included in the summation.

Because the focus of the present work is upon aqueous systems, we adopt a reference state of infinite dilution with respect to the solvent, water, as the convention for expressing the activity coefficients of solute species. The symbol f_i^* is used for the activity coefficient on this basis; thus, $f_i^* \rightarrow 1$ as $x_i \rightarrow 0$ in the pure solvent. For the solvent itself (denoted by subscript 1), $f_1 \rightarrow 1$ as $x_1 \rightarrow 1$, and for all solution components $f_i = a_i / x_i$, where a_i is the activity of component i.

Activity and osmotic coefficients in aqueous solution are commonly represented in molal units, and for convenience a number of conversions to the corresponding mole fraction quantities are now given. The activity of the solvent (a_1) is related to the rational osmotic coefficient g, mole fraction activity coefficient f_1, and molal osmotic coefficient ϕ by

$$\ln(a_1) = g \ln(x_1) = \ln(x_1) + \ln(f_1) \qquad (2)$$

$$\ln(a_1) = -(M_1/1000)\, \phi \sum_j m_j \qquad (3)$$

where M_1 is the molar mass (g mol^{-1}) of the solvent and

* To whom correspondence should be addressed.

0021-9568/95/1740-0043$09.00/0

m_j the molal concentration of solute species j. The stoichiometric osmotic coefficient, calculated from a_1 on the basis of complete dissociation of H_2SO_4 (to H^+ and SO_4^{2-}), is denoted by ϕ_{st}. The mole fraction activity coefficient f_j^* is related to the corresponding molal value (γ_j) by (*15*)

$$f_j^* = \gamma_j(1 + (M_1/1000)\sum_j m_j) \quad (4)$$

where the summation is over all solute species. The model treats strong electrolytes as fully dissociated in solution. Raman spectral studies have shown that the first dissociation of sulfuric acid ($H_2SO_4 \rightleftarrows H^+ + HSO_4^-$) is essentially complete at <40 mol kg^{-1} and 298.15 K (*16*). However, this is not the case for the second dissociation reaction involving the bisulfate ion, which must be considered explicitly:

$$HSO_4^-{}_{(aq)} \rightleftarrows SO_4^{2-}{}_{(aq)} + H^+{}_{(aq)} \quad (5)$$

$$^xK_{HSO_4} = a(H^+)a(SO_4^{2-})/a(HSO_4^-) = x(H^+)f_H^*x(SO_4^{2-})f_{SO_4}^*/(x(HSO_4^-)f_{HSO_4}^*) \quad (6)$$

where $^xK_{HSO_4}$ is the thermodynamic dissociation constant of HSO_4^- on a mole fraction basis and x and a denote mole fraction and activity, respectively.

The model equations for solvent and solute activity coefficients contain the cation–anion (ca) interaction parameters B_{ca}, $W_{1,ca}$, $U_{1,ca}$, and $V_{1,ca}$ where c is H^+ and a can be HSO_4^- or SO_4^{2-}. These parameters are functions of temperature and pressure. A series of additional terms exist to describe interactions between pairs of dissimilar cations (or anions) and an ion of opposite sign (*14*). However, these were found not to be needed here. Model equations for aqueous H_2SO_4 are given below:

$$\ln(f_1) = 2A_xI_x^{3/2}/(1 + \varrho I_x^{1/2}) - x(H)x(HSO_4)B_{H\cdot HSO_4} \times \exp(-\alpha_{H\cdot HSO_4}I_x^{1/2}) - x(H)x(SO_4)B_{H\cdot SO_4} \times \exp(-\alpha_{H\cdot SO_4}I_x^{1/2}) + (1 - x_1)(1/F)(2E_{HSO_4}W_{1,H\cdot HSO_4} + 1.5E_{SO_4}W_{1,H\cdot SO_4}) + (1 - 2x_1)x(H)(4x(HSO_4)U_{1,H\cdot HSO_4} + 4.5x(SO_4)U_{1,H\cdot SO_4}) + 4x_1(2 - 3x_1)x(H) \times (x(HSO_4)V_{1,H\cdot HSO_4} + x(SO_4)V_{1,H\cdot SO_4}) - 2x(HSO_4)x(SO_4)(\vartheta_{HSO_4,SO_4} + I_x\vartheta'_{HSO_4,SO_4}) \quad (7)$$

$$\ln(f_H^*) = -A_x((2/\varrho)\ln(1 + \varrho I_x^{1/2}) + I_x^{1/2}(1 - 2I_x)/(1 + \varrho I_x^{1/2})) + x(HSO_4)B_{H\cdot HSO_4}g(\alpha_{H\cdot HSO_4}I_x^{1/2}) + x(SO_4)B_{H\cdot SO_4} \times g(\alpha_{H\cdot SO_4}I_x^{1/2}) - x(H)x(HSO_4)B_{H\cdot HSO_4}(g(\alpha_{H\cdot HSO_4}I_x^{1/2})/(2I_x) + (1 - 0.5/I_x)\exp(-\alpha_{H\cdot HSO_4}I_x^{1/2})) - x(H) \times x(SO_4)B_{H\cdot SO_4}(g(\alpha_{H\cdot SO_4}I_x^{1/2})/(2I_x) + (1 - 0.5/I_x)\exp(-\alpha_{H\cdot SO_4}I_x^{1/2})) + 2x_1E_{HSO_4}(W_{1,H\cdot HSO_4} - (0.5 + 1/F)W_{1,H\cdot HSO_4}) + 1.5x_1E_{SO_4}(W_{1,H\cdot SO_4} - (0.5 + 1/F)W_{1,H\cdot SO_4}) + 4x_1x(HSO_4)U_{1,H\cdot HSO_4}(1 - 2x(H)) + 4.5x_1x(SO_4)U_{1,H\cdot SO_4}(1 - 2x(H)) + 4x_1^2x(HSO_4) \times V_{1,H\cdot HSO_4}(1 - 3x(H)) + 4x_1^2x(SO_4)V_{1,H\cdot SO_4}(1 - 3x(H)) - 2x(HSO_4)x(SO_4)(\vartheta_{HSO_4,SO_4} + \vartheta'_{HSO_4,SO_4}(I_x - 0.5)) - (E_{HSO_4}W_{1,H\cdot HSO_4} + 0.75E_{SO_4}W_{1,H\cdot SO_4}) \quad (8)$$

$$\ln(f_{HSO_4}^*) = -A_x((2/\varrho)\ln(1 + \varrho I_x^{1/2}) + I_x^{1/2}(1 - 2I_x)/(1 + \varrho I_x^{1/2})) + x(H)B_{H\cdot HSO_4}g(\alpha_{H\cdot HSO_4}I_x^{1/2}) - x(H)x(HSO_4)B_{H\cdot HSO_4}(g(\alpha_{H\cdot HSO_4}I_x^{1/2})/(2I_x) + (1 - 0.5/I_x)\exp(-\alpha_{H\cdot HSO_4}I_x^{1/2})) - x(H)x(SO_4)B_{H\cdot SO_4}(g(\alpha_{H\cdot SO_4}I_x^{1/2})/(2I_x) + (1 - 0.5/I_x) \times \exp(-\alpha_{H\cdot SO_4}I_x^{1/2})) + 2x_1(W_{1,H\cdot HSO_4} - (0.5 + 1/F) \times (E_{HSO_4}W_{1,H\cdot HSO_4} + 0.75E_{SO_4}W_{1,H\cdot SO_4})) + x_1x(H)(4 \times U_{1,H\cdot HSO_4}(1 - 2x(HSO_4)) - 9x(SO_4)U_{1,H\cdot SO_4}) + 4x_1^2x(H)(V_{1,H\cdot HSO_4} - 3x(HSO_4)V_{1,H\cdot HSO_4} - 3x(SO_4)V_{1,H\cdot SO_4}) + 2x(SO_4)(\vartheta_{HSO_4,SO_4} - x(HSO_4) \times (\vartheta_{HSO_4,SO_4} + \vartheta'_{HSO_4,SO_4}(I_x - 0.5))) - (2(1 - E_{HSO_4}/2) \times W_{1,H\cdot HSO_4} + 0.75E_{SO_4}W_{1,H\cdot SO_4}) \quad (9)$$

$$\ln(f_{SO_4}^*) = -4A_x((2/\varrho)\ln(1 + \varrho I_x^{1/2}) + I_x^{1/2}(1 - I_x/2)/(1 + \varrho I_x^{1/2})) + x(H)B_{H\cdot SO_4}g(\alpha_{H\cdot SO_4}I_x^{1/2}) - x(H)x(HSO_4)B_{H\cdot HSO_4}(2g(\alpha_{H\cdot HSO_4}I_x^{1/2})/I_x + (1 - 2/I_x) \times \exp(-\alpha_{H\cdot HSO_4}I_x^{1/2})) - x(H)x(SO_4)B_{H\cdot SO_4} \times (2g(\alpha_{H\cdot SO_4}I_x^{1/2})/I_x + (1 - 2/I_x)\exp(-\alpha_{H\cdot SO_4}I_x^{1/2})) + x_1(3W_{1,H\cdot SO_4} - (1 + 1/F)(1.5E_{SO_4}W_{1,H\cdot SO_4} + 2E_{HSO_4}W_{1,H\cdot HSO_4})) + x_1x(H)(4.5U_{1,H\cdot SO_4}(1 - 2x(SO_4)) - 8x(HSO_4)U_{1,H\cdot HSO_4}) + 4x_1^2x(H)(V_{1,H\cdot SO_4} - 3x(SO_4)V_{1,H\cdot SO_4} - 3x(HSO_4)V_{1,H\cdot HSO_4}) + 2x(HSO_4) \times (\vartheta_{HSO_4,SO_4} - x(SO_4)(\vartheta_{HSO_4,SO_4} + \vartheta'_{HSO_4,SO_4}(I_x - 2))) - (3(1 - E_{SO_4}/2)W_{1,H\cdot SO_4} + 2E_{HSO_4}W_{1,H\cdot HSO_4}) \quad (10)$$

In the above equations ionic charges have been omitted from the mole fractions for simplicity. Symbol I_x denotes the mole fraction ionic strength, given by $0.5\sum_i x_iz_i^2$, where z_i is the magnitude of the charge on ion i. The Debye–Hückel constant on a mole fraction basis, A_x, is related to the molal value A_ϕ ($mol^{-1/2}$ $kg^{1/2}$) by $A_x = (1000/M_1)^{1/2}A_\phi$. Over most of the temperature range we adopt values of the Debye–Hückel constant recently calculated by Archer and Wang (*17*), which are represented using a Chebychev polynomial. For temperatures below 273.15 K an empirical extension is used (see section 4). The necessary equations and temperature coefficients are given in Appendix 1.

Equivalent fractions E_a for anions HSO_4^- and SO_4^{2-} are defined by

$$E_a = x_az_a/(\sum_a x_az_a) \quad (11)$$

Also

$$F = 1/[(1/2)(\sum_c x_cz_c + \sum_a x_az_a)] \quad (12)$$

The values of parameters B_{ca}, $W_{1,ca}$, $U_{1,ca}$, and $V_{1,ca}$ in eqs 7–10 are determined by fitting to thermodynamic data. Coefficients $\alpha_{H\cdot HSO_4}$ and $\alpha_{H\cdot SO_4}$ are here given fixed values of 17.0 and 9.5, respectively, and ϱ is set equal to 13.0. Note that, for the four model parameters and coefficient α_{ca}, a dot has been inserted between cation and anion to distinguish between anion HSO_4^- and the interaction between

H^+ and SO_4^{2-}. The function $g(x)$ in eqs 8–10 is given by

$$g(x) = 2[1 - (1 + x)\exp(-x)]/x^2 \quad (13)$$

Functions ϑ_{ij} and ϑ'_{ij}, for two ions of the same sign but differing charge magnitude, are unsymmetrical mixing terms analogous to those appearing in the molality-based model of Pitzer (*18, 19*) and are given by

$$\vartheta_{ij} = (z_i z_j / 4I_x)[J(x_{ij}) - 1/2J(x_{ii}) - 1/2J(x_{jj})] \quad (14)$$

$$\vartheta'_{ij} = \partial\vartheta_{ij}/\partial I_x = -\vartheta_{ij}/I_x + (z_i z_j / 8I_x^2) \times [x_{ij}J'(x_{ij}) - (1/2)x_{ii}J'(x_{ii}) - (1/2)x_{jj}J'(x_{jj})] \quad (15)$$

and

$$J'(x_{ij}) = \partial J(x_{ij})/\partial x_{ij} \quad (16)$$

The concentration variable x_{ij} is given by

$$x_{ij} = 6 z_i z_j A_x I_x^{1/2} \quad (17)$$

Note that x_{ij} is not a mole fraction. The function $J(x_{ij})$ is an integral which must be evaluated numerically. The following approximating equation is used here to obtain values of $J(x_{ij})$ and $J'(x_{ij})$ (*18*):

$$J(x_{ij}) = x_{ij}/[4 + C_1 x_{ij}^{C_2}\exp(C_3 x_{ij}^{C_4})] \quad (18)$$

with $C_1 = 4.581$, $C_2 = -0.7237$, $C_3 = -0.0120$, and $C_4 = 0.528$. More accurate (but complex) methods are available (*19*).

Model equations for apparent molar enthalpy ($^\phi L$, J mol^{-1}) and heat capacity ($^\phi C_p$, J mol^{-1} K^{-1}) may be obtained by differentiation of the following excess Gibbs energy expression:

$$g^e/RT = x_1' \ln(f_1') + x_I' \ln(f_\pm^{*\prime}) \quad (19)$$

where g^e is the excess Gibbs energy per mole of particles and R is the gas constant (8.3144 J mol^{-1} K^{-1}). Variables x_1' and x_I' are the solvent mole fraction and total mole fraction of ions, respectively, expressed on the basis of complete dissociation of bisulfate; thus

$$x_1' = n_1/(n_1 + n(H^+) + 2n(HSO_4^-) + n(SO_4^{2-})) \quad (20)$$

$$x_I' = 1 - x_1' \quad (21)$$

The corresponding stoichiometric mean activity coefficient $f_\pm^{*\prime}$ and solvent activity coefficient f_1' are related to the quantities given by eqs 7, 8, and 10 by

$$f_1' = f_1(x_1/x_1') \quad (22)$$

$$f_\pm^{*\prime} = [(x(H^+)f_H^*)^2 f_{SO_4}^* x(SO_4^{2-})/(4(x_I')^3/27)]^{1/3} \quad (23)$$

Differentiation of eq 19 with respect to temperature, holding pressure and composition constant, yields the apparent molar enthalpy, $^\phi L$ (J mol^{-1})

$$^\phi L = -RT^2[\partial(g^e/RT)/\partial T]_{P,x}/(x_I'/3) \quad (24)$$

The apparent molar heat capacity, $^\phi C_p$ (J mol^{-1} K^{-1}), is similarly given by

$$^\phi C_p = {}^\phi C_p^\circ + \partial^\phi L/\partial T \quad (25a)$$

$$= {}^\phi C_p^\circ - RT[2\{\partial(g^e/RT)/\partial T\}_{P,x} + T\{\partial^2(g^e/RT)/\partial T^2\}_{P,x}]/(x_I'/3) \quad (25b)$$

where $^\phi C_p^\circ$ (J mol^{-1} K^{-1}) is the infinite dilution value of the apparent molar heat capacity, equivalent to the standard state heat capacity of the SO_4^{2-} ion (since by convention $C_p^\circ(H^+) = 0$). Because the dissociation of HSO_4^- is a function of temperature, expressions obtained by the analytical differentiation of eq 19 would be extremely complex. In this work we have therefore differentiated numerically to obtain the required quantities in the expressions for $^\phi L$ and $^\phi C_p$, using centered finite difference formulae incorporating either four (for $\partial/\partial T$) or five (for $\partial^2/\partial T^2$) terms. The step size was set to $1.6 \times 10^{-3} T$, where T is the temperature of the measurement.

The above equations, together with the dissociation constant ($^xK_{HSO_4}$) and an iterative technique to determine speciation (e.g., Brent's method (*20*)), enable solute and solvent activity coefficients and thermal properties to be calculated for any given set of model parameters.

3. Dissociation Constant ($^xK_{HSO_4}$) of the Bisulfate Ion

The value of $^xK_{HSO_4}$ (eq 6) is such that it is difficult to determine using methods employed for weaker acids, for example, electromotive f ce measurements (*21*). The double charge on the sulfate ion complicates the extrapolation of activity coefficients that is required, and renders this sensitive to model assumptions such as the value of the ion size parameter in the Debye–Hückel limiting law expression (*22, 23*). The many determinations of K_{HSO_4} (the molal equivalent of $^xK_{HSO_4}$) that have been made are summarized in a number of reviews (*24–26*). They are further discussed by Clegg *et al.* (*6*) whose expression for K_{HSO_4} as a function of temperature (transformed from the molality to mole fraction scale) we have adopted. It is based upon a 298.15 K value of 0.0105 mol kg^{-1}, determined previously by Pitzer *et al.* (*27*) and confirmed by later studies (*23, 28*), and a variation with temperature established by Dickson *et al.* (*26*), giving

$$\log(^xK_{HSO_4}) = 560.95050 - 102.5154\ln(T) - 1.117033 \times 10^{-4}T^2 + 0.2477538T - 13273.75/T \quad (26)$$

The value of $^xK_{HSO_4}$ at 298.15 K is 1.892×10^{-4}. Note that the numbers of significant figures given in eq 26 do not reflect the accuracy with which $^xK_{HSO_4}$ has been determined, but are retained to avoid cancellation of terms and maintain close agreement with thermal properties of the reaction (obtained by differentiation). Dickson *et al.* (*26*) determined $\Delta_r H^\circ$ equal to -22.8 ± 0.8 kJ mol^{-1}, and $\Delta_r C_p^\circ$ equal to -275 ± 17 J mol^{-1} K^{-1} for the dissociation reaction, both at 298.15 K. (The above equation, adapted from eq 6 of Dickson *et al.* (*26*), implies $\Delta_r H^\circ$ and $\Delta_r C_p^\circ$ equal to -22.755 kJ mol^{-1} and -274.877 J mol^{-1} K^{-1}, respectively, at 298.15 K.) These values are in reasonable agreement with earlier estimates, listed by Dickson *et al.* (*26*) and by Young and Irish (*24*) (for the enthalpy change only).

The quantity $\Delta_r C_p^\circ$ for the dissociation reaction is related to the apparent molar heat capacities of the ions at infinite dilution:

$$\Delta_r C_p^\circ = C_p^\circ(SO_4^{2-}) + C_p^\circ(H^+) - C_p^\circ(HSO_4^-) \quad (27)$$

By definition $C_p^\circ(H^+)$ is equal to 0; hence

$$\Delta_r C_p^\circ = C_p^\circ(SO_4^{2-}) - C_p^\circ(HSO_4^-) \quad (28a)$$

$$\equiv {}^\phi C_p^\circ - C_p^\circ(HSO_4^-) \quad (28b)$$

Values of $\Delta_r C_p^\circ$, derived from eq 26, have been shown to be consistent with estimates of ${}^\phi C_p^\circ$ (*6*) and the $C_p^\circ(HSO_4^-)$ calculated by Hovey and Hepler (*29*) for $T > 283.15$ K. At lower temperatures, particularly below 273.15 K, there are insufficient data to determine these quantities, although values of $\Delta_r C_p^\circ$ are of course implicit in eq 26, and ${}^\phi C_p^\circ$ is required as a parameter by the model at each temperature for which there are apparent molar heat capacities (to 240 K). For the present application we have assumed eq 26 to be valid over the full temperature range of the fit, and ${}^\phi C_p^\circ$ values at each temperature below 283.15 K have been fitted as unknowns.

4. Thermodynamic Properties of Aqueous H_2SO_4 below 273.15 K

The focus of the present study is upon solution properties at very low temperature. Our aims include the calculation of water vapor pressures over aqueous H_2SO_4 close to the freezing point—as low as 200 K—and ultimately the solubilities of other acids such as HCl and HNO_3 in aqueous H_2SO_4 at these temperatures. However, there are a number of specific problems regarding the real (and hypothetical) properties of pure water below 273.15 K that affect both practical calculations and the interpretation of data.

Speedy (*30*) has examined measured thermodynamic properties of liquid water (density, heat capacity, and isothermal compressibility) from +150 to −38 °C, and found them to be consistent with a singularity at −46 °C (227.15 K). The heat capacity, for example, tends to infinity at this temperature which may represent the limit of mechanical stability of the supercooled liquid phase. By contrast, in aqueous solutions such as sulfuric acid which can remain liquid below −46 °C, there is no evidence of such a singularity, presumably because the structural properties of water in the solution are greatly altered by the presence of the ions. Thus, there is the problem of defining appropriate, and self-consistent, values of pure water properties for use below 273.15 K.

The following properties of supercooled water are needed for data analysis, and use of the model equations.

(a) The Debye–Hückel constant (A_x). This is a function of solvent density (to the power 1/2) and dielectric constant (to the power −3/2), and has been evaluated to 238.15 K by Archer and Wang (*17*) from measurements including the water density equation of Speedy (*30*). The Debye–Hückel constant and limiting law expression, of which it is a part, describe solution properties at extreme dilution. Since solutions have to be fairly concentrated to remain liquid at temperatures significantly below 273.15 K, and the Debye–Hückel limiting slopes are not approached, the values of A_x and its derivatives are not critical in terms of properties calculated using the model. However, the choices made do affect the values of the various short-range interaction parameters, because of the nature of the model (correlation between short- and long-range elements of the expressions).

We have adopted the Debye–Hückel constant of Archer and Wang (*17*) to a low-temperature limit of 273.15 K. Values were obtained using a program supplied by Donald Archer, and are here represented by a Chebychev polynomial; see Appendix 1. Below 273.15 K, Debye–Hückel constants used in model calculations were based upon a linear extrapolation of A_{Cx}, to retain continuity in model-calculated thermal properties. (A_{Cx}, the Debye–Hückel heat capacity parameter is equal to $4RT(2[\partial A_x/\partial T]_P + T[\partial^2 A_x/\partial T^2]_P)$.) The following equation gives A_x for $T \leq 273.15$ K:

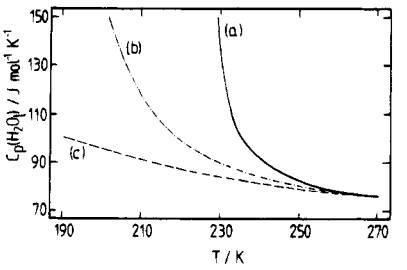

Figure 1. Heat capacity of (supercooled) liquid water below 273.15 K: (a) from Speedy's equation (*30*), based on experimental measurements; (b) inferred from the Goff–Gratch formula for the vapor pressure of supercooled liquid water (*35*); (c) obtained by extrapolating Hill's equation of state (*34*) and used in the calculation of ϕ_{fr} and ${}^\phi C_p$ in this study.

$$A_x = A + B(1/T_r - 1/T) + C(\ln(T/T_r) + T_r/T - 1) + D(T - T_r^2/T - 2T_r \ln(T/T_r)) \quad (29)$$

where T_r is the reference temperature of 273.15 K and T (K) is the temperature of interest. Values of constants A–D, and the basis of the derivation, are given in Appendix 1.

(b) The heat capacity of pure water ($C_p(H_2O_{(l)})$, J mol^{-1} K^{-1}). This is required, first, to calculate the apparent molar heat capacity ${}^\phi C_p$ of H_2SO_4 in solution, which we have analyzed to 240 K (Appendix 2, section d). Second, $C_p(H_2O_{(l)})$ is also implicit (as $[C_p(H_2O_{(l)}) - C_p(H_2O_{(s)})]$ for the equilibrium $H_2O_{(s)} \rightleftarrows H_2O_{(l)}$) in the standard equations used to obtain osmotic coefficients from freezing point data (*31, 32*). Third, a hypothetical partial pressure for pure supercooled liquid water is required to estimate vapor pressures of water over aqueous H_2SO_4 or other solutions, where the water activity is first calculated by the model. Any extrapolation that is used for this must assume values of $\Delta_r C_p^\circ$ for the equilibrium $H_2O_{(l)} \rightleftarrows H_2O_{(g)}$.

Use of measured $C_p(H_2O_{(l)})$ in the equation used to transform heat capacity data, and freezing point measurements, is only possible to about 230 K. As previously noted, it is unlikely that the observed behavior of supercooled water corresponds to that of the water component of aqueous solutions, since solution properties (e.g., solid phase precipitation, vapor pressures (*33*)) vary smoothly with temperature down to at least 200 K. In this work we have adopted values of $C_p(H_2O_{(l)})$ below 273.15 K calculated from an extrapolation of Hill's equation of state for water (*34*). This is based on $C_p(H_2O_{(l)})$ equal to 75.994 J mol^{-1} K^{-1} at 273.15 K, and first and second differentials with respect to temperature of −0.064 242 J mol^{-1} K^{-2} and 5.405 × 10^{-3} J mol^{-1} K^{-3}; see section d of Appendix 2.

In Figure 1 we compare $C_p(H_2O_{(l)})$ calculated from the equation of Speedy (*30*), extrapolated from the equation of state of Hill (*34*) as described above, and also derived from the Goff–Gratch formula (*35*). The latter is a thermodynamically consistent equation for the partial pressure of supercooled liquid water, based upon data above the freezing point, and often used in practical calculations in the field of meteorology. We note also that the equation relating freezing point depression to water activity at the freezing temperature, presented by Klotz (*32*) and based

Table 1. Osmotic Coefficients (ϕ_{fr}) Calculated from Freezing Point Depression Data (44)[a]

T/K	$m(H_2SO_4)$	ϕ_{fr}[b]	ϕ_{fr}[c]	ϕ_{fr}[d]
270.88	0.5781	0.7049	0.7049	0.7049
269.31	0.9370	0.7363	0.7363	0.7363
268.01	1.2226	0.7557	0.7557	0.7557
266.14	1.5647	0.8059	0.8060	0.8060
262.86	2.0817	0.8903	0.8903	0.8903
258.67	2.6264	0.9941	0.9940	0.9941
253.20	3.2045	1.124	1.123	1.124
248.49	3.6251	1.228	1.229	1.228
244.34	3.9444	1.318	1.316	1.318
238.81	4.3269	1.431	1.425	1.430
231.97	4.7601	1.555	1.539	1.553
228.17	4.9369	1.634		1.630
223.71	5.1432	1.719		1.713
218.53	5.3611	1.813		1.803
213.92	5.5584	1.886		1.872
211.24	5.6605	1.929		1.911
207.84	5.8130	1.972		1.949
203.93	5.9528	2.028		1.997
201.94	6.0188	2.056		2.021

[a] All water activities at the freezing temperature T (K), and hence ϕ_{fr}, were calculated using the standard equation (see Young (31), and eq 21-88 of Klotz (32)), which gives $\log(a_1)$ in terms of a polynomial in the freezing point depression, ϑ. In each of the three cases above, the coefficients were calculated (31) from the same 273.15 K values of $\Delta_r H°$ and $\Delta_r C_p°$ for the fusion of ice, and different low-temperature values of $C_p(H_2O_{(l)})$ as indicated below. Measured values (108) of the heat capacity of ice were used. [b] $C_p(H_2O_{(l)}) = 104.34 - 0.10464T$ J mol^{-1} K^{-1}. This relationship was derived from eq 21-88 of Klotz (32), which is based upon the original work of Young (31). [c] $C_p(H_2O_{(l)})$ from Speedy's equation (30). Note that there is a typographical error in the published paper: the term $+ C_x^{-1/2}$ in Speedy's eq 13 should be $+ C_x e^{-1/2}$. [d] $C_p(H_2O_{(l)})$ extrapolated from Hill's equation of state (34) using the value at 273.15 K together with first and second differentials with respect to temperature, also at 273.15 K (see section d of Appendix 2).

upon the work of Young (31), implies a slow linear change of $C_p(H_2O_{(l)})$ with T below 273.15 K to about 85 J mol^{-1} K^{-1} at 190 K. The influence of differing $C_p(H_2O_{(l)})$ values on calculated osmotic coefficients at the freezing point of the solution (ϕ_{fr}) are shown in Table 1. Even at 201 K the differences in ϕ_{fr} are less than 5%. In view of this, and the small number of freezing point data at very low temperature, it is unlikely that the choice of $C_p(H_2O_{(l)})$ will have a significant effect on the overall analysis in terms of ϕ_{fr}.

Comparisons of apparent molar heat capacities calculated using $C_p(H_2O_{(l)})$ given by Speedy's equation (30), and the Hill-based values, show deviations on the order of 12 J mol^{-1} K^{-1} at 253.15 K and 35 J mol^{-1} K^{-1} at 240 K (after accounting for the differing $^{\phi}C_p°$ values), which are quite large. However, apparent molar heat capacities relate only to the second differential of activity with respect to temperature, and test calculations indicated that the use of sets of apparent molar heat capacities (below 273.15 K) based upon different assumed $C_p(H_2O_{(l)})$ had only a small influence on the fitted model.

What effect do different values of $C_p(H_2O_{(l)})$ have on estimates of water vapor pressures over supercooled liquid water? Table 2 shows partial pressures calculated from the Goff–Gratch formula, and those arising from the substitution of $C_p(H_2O_{(l)})$ based on the extrapolation described above. At 190 K, close to the lower limit of temperature in the polar winter stratosphere, the difference is only about 15%. There is also a test of consistency among the vapor pressures of H_2O above supercooled liquid water ($p°(H_2O_{(l)})$) and ice ($p(H_2O_{(s)})$), and the water activity of aqueous H_2SO_4 at the freezing temperature of the

Table 2. Estimated Partial Pressures (atm) of H_2O over Supercooled Liquid Water

T/K	$p°(H_2O)_{(l)}$[a]	$p°(H_2O)_{(l)}$[b]	Δ[c]/%
273.15	6.03×10^{-3}	6.03×10^{-3}	0.0
270.00	4.78×10^{-3}	4.78×10^{-3}	0.0
260.00	2.19×10^{-3}	2.19×10^{-3}	0.01
250.00	9.39×10^{-4}	9.39×10^{-4}	0.03
240.00	3.71×10^{-4}	3.71×10^{-4}	0.05
230.00	1.34×10^{-4}	1.34×10^{-4}	0.05
220.00	4.34×10^{-5}	4.35×10^{-5}	−0.07
210.00	1.24×10^{-5}	1.25×10^{-5}	−0.55
200.00	3.07×10^{-6}	3.13×10^{-6}	−1.95
190.00	6.27×10^{-7}	6.62×10^{-7}	−5.62
180.00	1.00×10^{-7}	1.15×10^{-7}	−14.8

[a] Calculated from the Goff–Gratch formula, as given by McDonald (35). [b] Calculated using values of the vapor pressure, $\Delta_r H°$, and $\Delta_r C_p°$ at 273.15 K consistent with Goff–Gratch, but $C_p(H_2O_{(l)})$ given by eq A2.6, and $C_p(H_2O_{(g)})$ obtained from the JANAF tables (109). [c] Percentage difference of calculated partial pressure (third column) from the Goff–Gratch value (second column).

solution (a_1):

$$a_1 p°(H_2O_{(l)}) = p(H_2O_{(s)}) \qquad (30)$$

At the lowest freezing temperature (201.94 K), we can compare the water activity calculated from ϕ_{fr} (Table 1, column 5) with the ratio of partial pressures obtained using the Goff–Gratch formula for $p(H_2O_{(s)})$, and an equivalent equation for $p°(H_2O_{(l)})$ modified to include our extrapolation of $C_p(H_2O_{(l)})$. There is agreement to within 9×10^{-4} in a_1 (0.2%), a satisfactory result.

In summary, values of the Debye–Hückel parameter A_x, and its derivatives with respect to temperature, are based upon an extrapolation below 273.15 K. Modeled solution properties are not thought to be sensitive to this, as freezing prevents the solutions from becoming dilute enough to approach limiting law slopes. Heat capacities of pure supercooled water based upon the Hill equation of state (34), also extrapolated below 273.15 K, have been adopted to analyze low-temperature heat capacities and freezing points (solid phase ice) of aqueous H_2SO_4. Comparisons of osmotic coefficients at the freezing points of the solutions, and test fits of the model using sets of apparent molal heat capacities (below 273.15 K) based upon different heat capacities of pure water, suggest that the choice is not critical.

5. Data

There is a very large body of experimental measurements relating to aqueous H_2SO_4, dating back at least a century. Early work is summarized in compilations by Bichowsky and Rossini (36) and Timmermans (37). Sources of data have been compiled by Staples and Wobbeking (1) and Staples *et al.* (38). Previous evaluations of the thermodynamic properties of aqueous H_2SO_4 include those of Giauque and co-workers (39) (0–100% acid; $T \leq 300$ K), Pitzer *et al.* (27) (0–6 mol kg^{-1}; temperatures at, or close to, 298.15 K), Staples (2) (0–28 mol kg^{-1}; 298.15 K), Rard *et al.* (3) (0.1–27.7 mol kg^{-1}; 298.15 K) with later improvements (40, 41), and Zeleznik (5) (0–100% acid; $200 \leq T \leq 350$ K but excluding vapor pressures). Vapor–liquid equilibrium in the H_2SO_4–H_2O system, with an emphasis on high temperatures, has been evaluated by Gmitro and Vermeulen (42) and Bolsaitis and Elliott (4). Recently, Clegg *et al.* (6) have examined osmotic coefficient, emf, bisulfate dissociation, and thermal data for $m(H_2SO_4)$ below 6.0 mol kg^{-1}. Much of their discussion is relevant to the present study, particularly the assignment of weights, and

Table 3. Thermodynamic Data Fitted by the Model

measurement	quantity fitted	symbol	data table
isopiestic	osmotic coefficient[a]	ϕ_{st}	11
direct vapor pressure	osmotic coefficient[a]	ϕ_{st}	11
electromotive force	measured emf	E	12
enthalpy	differential heat of dilution	$\Delta_{dil}H$	13
	partial molar enthalpy of water[b]	$L(H_2O)$	13
heat capacity	apparent molar heat capacity	${}^{\phi}C_p$	14
dissociation of HSO_4^-	degree of dissociation	α	15
freezing point depression	osmotic coefficient at the freezing temperature[a]	ϕ_{fr}	16
saturation with respect to $H_2SO_4{\cdot}4H_2O$	activity product difference[c]		16

[a] In all cases the molal quantity (ϕ_{st} or ϕ_{fr}) was fitted. [b] Values for $T \leq 245.15$ K, generated from equations given by Zelenik (*5*). [c] For much of the temperature range over which aqueous H_2SO_4 becomes saturated with respect to the tetrahydrate, there are two compositions (at each value of T) for which saturation occurs. The activity products, defined in section 7, must be the same at each composition, and the difference is therefore 0. See Appendix 2 (section f) for further discussion.

readers are referred to this work for information additional to that presented here.

The types of experimental data used in the present correlation are listed in Table 3, and considered in detail in Appendix 2. Tables 11–16 list, for each data type, the concentration and temperature ranges of measurement from each source, the numbers of experimental points, measurements rejected as being in error, and the relative weight assigned to each data set. Below about 240 K, the only measurements are freezing points with respect to ice (to 201 K) and $H_2SO_4{\cdot}4H_2O$ (245–221 K), which constrain the model poorly (even though they are fitted well). It was therefore decided to include partial molal enthalpies of water ($L(H_2O)$, J mol^{-1}) for $T \leq 245.15$ K in the overall data set; see Table 13. The enthalpies were calculated using the equations of Zeleznik (*5*), whose evaluation of the properties of aqueous H_2SO_4 was found to agree well with the model at higher temperatures.

6. Method

The sets of parameters B_{ca}, $W_{1,ca}$, $U_{1,ca}$, and $V_{1,ca}$ must be determined as functions of temperature so as to minimize the total sum of squared deviations for the measured properties ϕ_{st}, ϕ_{fp} (osmotic coefficients at the freezing temperature of the solution), emf, $\Delta_{dil}H$, ${}^{\phi}C_p$, α, the activity product difference for $H_2SO_4{\cdot}4H_2O$, and also partial molal enthalpies of water. This was done using a generalized nonlinear least-squares fitting routine (E04FDF (*43*)), first obtaining estimates of the 298.15 K parameter values from ϕ_{st} and emf data and then extending the fit to 298.15 K thermal data and finally to emf, ${}^{\phi}C_p$, and other measurements over the full temperature range. The use of different temperature functionalities for the parameters was explored.

Sulfate–bisulfate speciation is, of course, not known *a priori* and was calculated for every data point for each successive set of parameter estimates. This was done by determining the zero of the following function $\boldsymbol{F}$, which describes the distribution of the total hydrogen ion concentration in solution between free H^+ ($x(H^+)$) and HSO_4^- ($x(HSO_4^-)$):

$$\boldsymbol{F} = x(H^+)(x(SO_4^{2-}) + x(HSO_4^-))/({}^{x}K_{HSO_4}{}^{*} + x(H^+)) - x(HSO_4^-) \quad (31)$$

where ${}^{x}K_{HSO_4}{}^{*}$ is the stoichiometric dissociation constant of the bisulfate ion, equivalent to ${}^{x}K_{HSO_4}f_{HSO_4}{}^{*}/(f_H{}^{*}f_{SO_4}{}^{*})$. Because the incremental change in parameter estimates during the fitting process may be very small, and the fact that heats of dilution and heat capacities are calculated as numerical differentials (eqs 24 and 25), it was necessary to determine speciation to full machine precision (typically 1 part in 10^{16}).

The relative weights (w_r) assigned to measurements from different sources for each data type do not take into account the differing magnitudes of experimental error—about 1.5 J mol^{-1} K^{-1} in the case of ${}^{\phi}C_p$ compared with only 1.3×10^{-4} V for the emf measurements. The absolute weight given to an individual data point in the model fit is therefore set equal to the relative weight multiplied by a characteristic weight (w_c) for each type of data. Initially these were set so as to give contributions to the total sum of squared deviations approximately in the ratio 3:2:1:1:0.25 (ϕ_{st}:emf:$\Delta_{dil}H$:${}^{\phi}C_p$:α, with $H_2SO_4{\cdot}4H_2O$ saturation excluded). As the fit of the model was refined, the characteristic weights were recalculated as

$$w_c = [(10/N)\sum w_r(y - \boldsymbol{f})^2]^{-1} \quad (32)$$

where y and $\boldsymbol{f}$ are observed and fitted quantities, respectively, and N is the number of points (for which $w_r \neq 0$) in each data set. Some minor adjustments to w_c were later made—increasing the weight given to $\Delta_{dil}H$ and decreasing that assigned to ${}^{\phi}C_p$ by small amounts. The characteristic weights, w_c, assigned to each data set are as follows: ϕ_{st}, 1.94×10^4; $H_2SO_4{\cdot}4H_2O$ saturation, 0.064; emf, 1.46×10^6; $\Delta_{dil}H$, 2.43×10^{-4}; ${}^{\phi}C_p$, 2.37×10^{-2}; α, 49.8; ϕ_{fp} 2.425×10^3. The standard errors (σ) equivalent to these w_c are $\sigma(\phi_{st}) = 0.0023$, $\sigma(H_2SO_4{\cdot}4H_2O) = 1.25$, $\sigma(\text{emf}) = 2.6 \times 10^{-4}$ V, $\sigma(\Delta_{dil}H) = 20.3$ J mol^{-1}, $\sigma({}^{\phi}C_p) = 2.1$ J K^{-1} mol^{-1}, $\sigma(\alpha) = 0.045$, and $\sigma(\phi_{fp}) = 0.0064$. (Note that these standard errors will not be representative of fits to data with relative weights (w_r) significantly less than unity.) Values of the partial molal enthalpy of water that were included in the fit were assigned w_c equal to 1×10^{-6}, to ensure a relatively small influence (4% of the total sum of squared deviations).

7. Results

The general equation for the temperature variation of model parameter P is given below:

$$P = q_1 + (T - T_r)(0.1q_2 + (T - T_r)(10^{-2}q_3/2 + (T - T_r)(10^{-3}q_4/6 + (T - T_r)10^{-3}q_5/12))) \quad (33)$$

where T is in kelvin and the reference temperature T_r is 328.15 K. All parameters determined in the model fit are listed in Table 4, together with the individual ${}^{\phi}C_p{}^{\circ}$ for $T \leq 280$ K, and associated standard errors (see Appendix 2, section d, for further comment). For convenience, 298.15 K values of all parameters, including standard potentials of the electrochemical cells, are listed in Table 5. We note that the speciation (i.e., the degree of dissociation of bisulfate) is not uniquely determined by activity data alone.

Table 4. Fitted Model Parameters for Aqueous H_2SO_4[a]

	$B_{H\cdot HSO_4}$	$W_{1,H\cdot HSO_4}$	$U_{1,H\cdot HSO_4}$	$V_{1,H\cdot HSO_4}$
q_1	17.833 446 7	−9.984 163 90	−1.432 383 71	−2.074 745 66
q_2	−6.252 686 29	0.348 821 776	−0.201 636 224	0.594 737 744
q_3	0.591 429 323	−0.011 952 617 2	−0.044 380 423 2	0.067 405 222 1
q_4	0.223 751 841	0.009 094 256 62	0.006 418 478 19	0.0
q_5	0.0	0.000 149 166 944	0.000 296 327 801	−0.000 394 845 016
	$B_{H\cdot SO_4}$	$W_{1,H\cdot SO_4}$	$U_{1,H\cdot SO_4}$	$V_{1,H\cdot SO_4}$
q_1	−98.240 870 1	−10.775 215 5	−13.360 346 4	3.101 219 97
q_2	−20.540 180 6	−0.879 298 257	−4.594 795 78	4.461 890 09
q_3	−2.071 372 92	−0.440 528 485	−1.462 203 46	0.975 254 718
q_4	−0.037 652 193 7	−0.054 491 392 7	−0.157 872 023	0.005 887 482 31
q_5	−0.013 968 975 8	−0.000 173 541 364	−0.000 162 230 945	−0.000 901 983 372

T/K	${}^{\phi}C_p^{\circ}$	std error	T/K	${}^{\phi}C_p^{\circ}$	std error
280.0	−369.6	2.4	253.15	−515.0	11.7
270.0	−421.2	5.2	250.0	−535.4	13.0
260.0	−476.3	8.8	240.0	−595.6	17.6

[a] The coefficient $\alpha_{H\cdot HSO_4}$ is equal to 17.0, and $\alpha_{H\cdot SO_4}$ is equal to 9.5 at all temperatures. Mixture parameters (which involve all three ions) are set to 0. ${}^{\phi}C_p^{\circ}$ (J mol^{-1} K^{-1}) for 283.15 ≤ T ≤ 328.15 K, determined by Clegg *et al.* (*6*), are given by eq A2.7. The values listed above were fitted individually.

Table 5. Model Parameters and Standard Potentials at 298.15 K[a]

$B_{H\cdot HSO_4}$	38.246 054 2	$B_{H\cdot SO_4}$	−46.714 977 4
$W_{1,H\cdot HSO_4}$	−11.115 271 4	$W_{1,H\cdot SO_4}$	−9.886 201 69
$U_{1,H\cdot HSO_4}$	−1.036 067 97	$U_{1,H\cdot SO_4}$	−5.456 401 11
$V_{1,H\cdot HSO_4}$	−3.582 287 43	$V_{1,H\cdot SO_4}$	−5.983 181 62
$\alpha_{H\cdot HSO_4}$	17.0	$\alpha_{H\cdot SO_4}$	9.5
${}^{\phi}C_p^{\circ}$	−286.2		
E°(cell I)	1.691 00		
E°(cell II)	0.612 357		
E°(cell III)	1.077 55	A_x	2.91665
E°(cell IV)	0.352 768	${}^{x}K_{HSO_4}$	1.89159 × 10^{-4}

[a] The standard potentials of cells I–IV (E°, V) and the infinite dilution value of the apparent molal heat capacity (${}^{\phi}C_p^{\circ}$, J mol^{-1} K^{-1}) are fixed at the values determined by Clegg *et al.* (*6*).

At low temperatures there are relatively few measurements, and it proved possible to obtain fits with different trends of α with temperature at high molalities, but with similar overall sums of squared deviations. The result presented here was adopted on the basis of simplicity (little change with temperature), and test calculations using data for HNO_3/H_2SO_4 and HCl/H_2SO_4 aqueous solutions.

Figures 2–7 show the residuals for each data set, excluding $L(H_2O)$. While some cyclic deviations of the residuals are evident for most data types, they are not large considering the range of concentration of the fit. Comparisons of $\Delta\phi_{st}$ (Figure 2) with the same quantity obtained in the 0–6 mol kg^{-1} fit using the molality-based Pitzer model (*6*) show a very similar pattern of residuals, with an increase in the range of $\Delta\phi_{st}$ of <0.002 for the present study. Differences between the two models, in terms of ϕ_{st}, over the 0–6 mol kg^{-1} molality range are as follows: −0.006, +0.004 (273.15 K), −0.0018, +0.0023 (298.15 K), and −0.0028, +0.0004 (323.15 K). The quality of fit achieved for the emf measurements for cells I–IV is very similar for both studies. Degree of dissociation data are relatively poorly fitted at molalities greater than about 10 mol kg^{-1} (Figures 6 and 15). The same trend (toward lower than measured values) is found even when the maximum concentration of fit is reduced. Although the reason for this is unclear, it is unlikely to prove a problem since species activities, rather than concentrations, are of primary interest. In the case of differential heats of dilution, deviations are here greater by up to a factor of 2 in dilute solutions (0.5–0.6 mol kg^{-1}) compared to the earlier study (*6*). Comparisons of partial molal enthalpies of H_2SO_4 ($L(H_2SO_4)$, Table 7) with values derived from the molality-based model (*6*) show agreement to within 353 J mol^{-1} (1.7%) at 298.15 K, 2085 J mol^{-1} (8.3%) at 273.15 K, and 1851 J mol^{-1} (3.7%) at 323.15 K. At the latter two temperatures the greatest deviations occur at the highest molalities; thus, for example, below 4 mol kg^{-1} at 323.15 K the two models agree to within 1.2%.

The heat capacity data are fitted well at all temperatures except 240 K. However, these data were given a reduced weight, and at this temperature it is likely that parameter values are primarily determined by the saturation data for $H_2SO_4{\cdot}4H_2O$, which are fitted well (Figure 7), and to a lesser extent by $L(H_2O)$. Calculated solute and solvent activities vary as smooth functions of temperature to 180 K, well below the likely limit of supercooling of the aqueous solutions. Relative partial molar heat capacities of H_2SO_4 at 298.15 K ($J(H_2SO_4)$, Table 7) agree with values obtained by Clegg *et al.* (*6*) to within 2.4%, with a maximum deviation of 9 J mol^{-1} K^{-1}.

Since, with the molality-based model, it was not possible to include $\Delta_{dil}H$ or ${}^{\phi}C_p$ data below 273.15 K because of the 6 mol kg^{-1} upper limit of fit, at temperatures below 273.15 K it is likely that the present model is more reliable. Aqueous solutions of H_2SO_4 can become saturated with respect to five different hydrates above 215 K and at concentrations of less than 40 mol kg^{-1}. For practical applications of the model to mixtures, where precipitation of these solid phases needs to be estimated, each saturated solution activity product must be known as a function of temperature. The activity product for a saturated solution in equilibrium with the pure solid phase $H_2SO_4{\cdot}nH_2O$ is given by $(a(H^+))^2a(SO_4^{2-})a_1^n$, and is equivalent to the equilibrium constant for the dissolution reaction:

$$H_2SO_4{\cdot}nH_2O_{(s)} \rightleftharpoons 2H^+_{(aq)} + SO_4^{2-}{}_{(aq)} + nH_2O_{(l)} \quad (34)$$

Values of the activity products of the different hydrates have been calculated, using the model, for each of the measured freezing points of Gable *et al.* (*44*) and Kunzler and Giauque (*45*) and then fitted as simple functions of temperature. Equations and parameters for each hydrate are listed in Table 6. Fitted molalities and temperatures of the saturated solutions are compared with the original data in Figure 8, and agree well.

For convenient reference, Table 7 lists calculated values of activity and osmotic coefficients, thermal properties, and

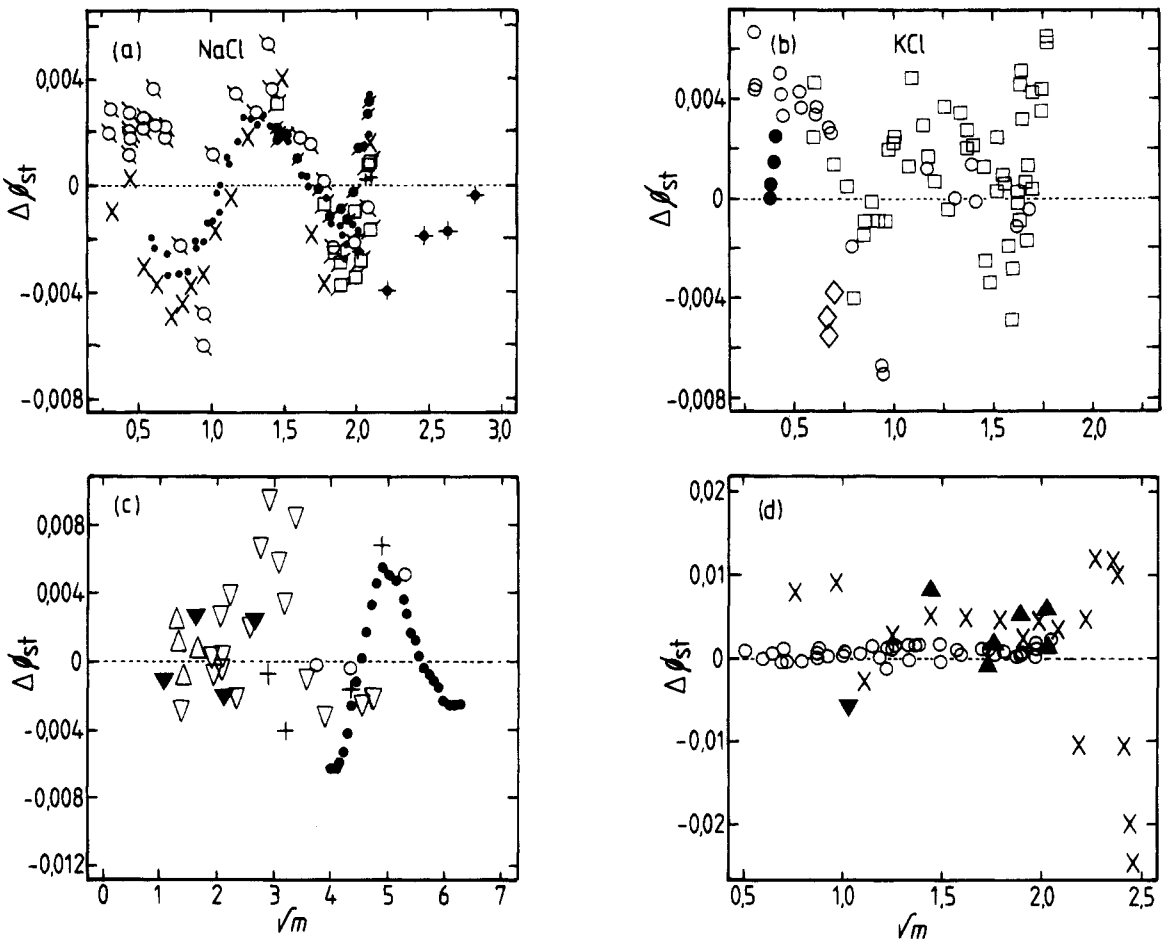

Figure 2. Deviations between the measured and fitted stoichiometric osmotic coefficients (ϕ_{st}) of aqueous H_2SO_4 at 298.15 K (a–c) and 273.15 and 323.15 K (d, which also shows the results for ϕ_{fr}): (a) aqueous NaCl used as osmotic coefficient standard, except for $N = 1$ (NaOH); (b) aqueous KCl used as osmotic coefficient standard; (c) direct vapor pressure measurements and evaluated osmotic coefficients of Giauque *et al.* (*39*). Sources (N in Table 11): (a) open square with diagonal, 2; ×, 3; open circle with diagonal, 5; ●, 11; dot with diagonal, 14; +, 23; dot with plus, 1; (b) ○, 4; □, 6; ●, 15; ◇, 16; (c) ▽, 7; △, 8; ○, 9; ▼, 12; +, 13; ●, 22; (d) ○, 17; ▲, 18; ▼, 19; ×, ϕ_{fr}.

degrees of dissociation at four temperatures from 253.15 to 323.15 K. Relative partial molar heat capacities of the solution components, in addition to enthalpies, are listed only at 298.15 K because the model is well constrained by measured heat capacities at this temperature. This is not the case at higher temperatures, and below 273.15 K a small uncertainty must also be introduced, related to the assumed heat capacity of pure water (section 4). Osmotic coefficients (ϕ_{st}) for a range of aqueous concentrations to very low temperature are also shown in Figure 9. Saturation with respect to the different solid phases is also indicated.

8. Comparisons with Other Studies

Zeleznik (*5*) has correlated the thermodynamic properties of aqueous H_2SO_4 and its related solid phases, as functions of temperature, over the entire concentration range. His approach is quite different from ours in terms of both the equations used and the treatment of the solution phase (dissociation of H_2SO_4 and HSO_4^- is not considered). However, it is based on much of the same data although, notably, Zeleznik excludes both isopiestic and direct vapor pressure measurements. Partial molar enthalpies of water, calculated from Zeleznik's equations (*5*), have been used to help constrain the present model at low temperature (see section 5 and Table 13). In Figure 10 we compare osmotic coefficients and water activities calculated by the present model with values derived from chemical potentials tabulated by Zeleznik (*5*) at 298.15, 250, and 200 K. Differences between the models are negligible for H_2SO_4 concentrations below 10 mol kg^{-1}. At 298.15 K, deviations remain below ±5% for $m(H_2SO_4)$ < 30 mol kg^{-1}, but increase to about +13% at the maximum molality of fit. This is probably due to the fact that our model is constrained at 298.15 K to isopiestic and vapor pressure data, including the evaluations of Giauque *et al.* (*39*), whereas this is not the case for Zeleznik's correlation.

Aqueous H_2SO_4 remains liquid to about 32 mol kg^{-1} at 250 K, and is saturated with respect to ice or $H_2SO_4 \cdot nH_2O$ at all molalities at 200 K. Deviations between the models are larger at these temperatures, reaching about +15% for the saturated solution (with respect to $H_2SO_4 \cdot H_2O$) at 250 K. Both enthalpies of dilution and heat capacities for $T \geq$ 253.15 K are fitted well by the present model, and at 250 K it is difficult to assess which of the two models is more nearly correct. Close to 200 K the present model is constrained mainly by freezing point data (for saturation with respect to ice and, for 221.35 K ≤ T ≤ 244.74 K, $H_2SO_4 \cdot 4H_2O$), and differences from the results of Zeleznik (expressed as percentages) become large at high molalities. In terms of a_1 directly, these differences amount to 5.1 × 10^{-3} at 10 mol kg^{-1} and about 2.6 × 10^{-4} at 40 mol kg^{-1}, for example.

The work of Zhang *et al.* (*33*) is particularly relevant to the thermodynamics of the stratospheric aqueous H_2SO_4 aerosol, as these authors have measured $p(H_2O)$ over H_2SO_4 solutions from 250 to almost 200 K. While the original

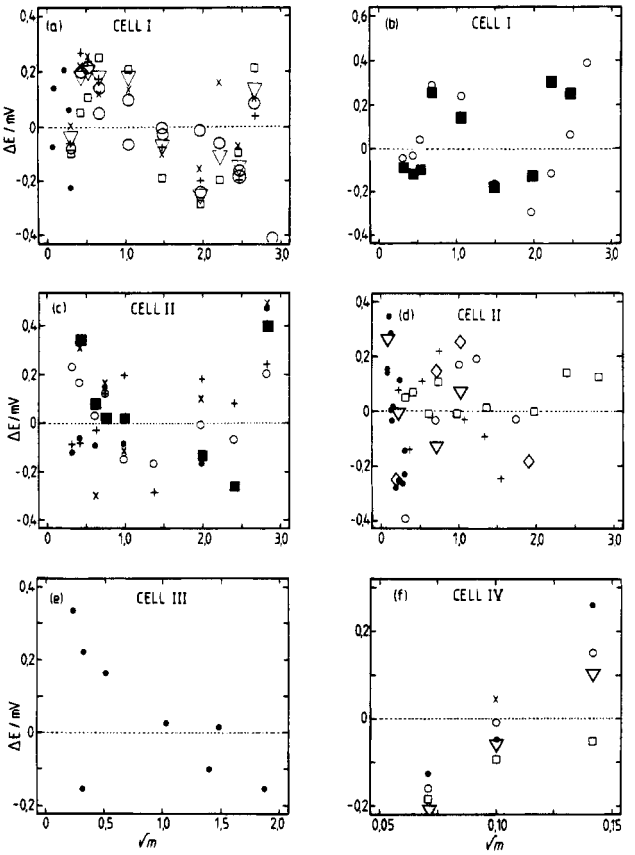

Figure 3. Deviations between measured and fitted emfs of cells I–IV. Temperatures (K): (a) ×, 278.15; +, 283.15; ▽, 293.15; ●, ○, 298.15; □, 308.15; (b) ○, 318.15; ■, 328.15; (c) ●, 278.15; +, 288.15; ○, 308.15; ■, 318.15; ×, 328.15; (d) 298.15; (e) 298.15; (f) ×, 273.15; ●, 285.65; ○, 298.15; ▽, 310.65; □, 323.15. Sources (N in Table 12): (a) ●, 2; all other symbols, 1; (b) 1; (c) 5; (d) □, 5; ●, 6; +, 7; ◇, 8; ▽, 10; ○, 11; (e) 12; (f) 13.

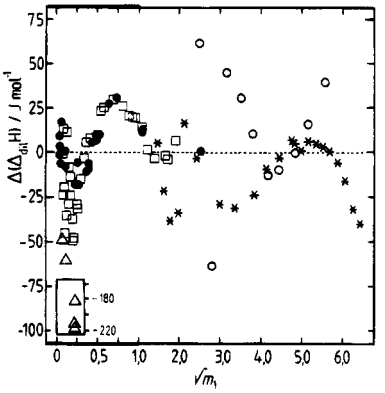

Figure 4. Deviations between measured and fitted differential heats of dilution at 298.15 and 253.15 K plotted against the square root of the initial molality m_1. Note the scale expansion at low concentration. Sources (N in Table 13): *, 1; ●, 2; □, 3; △, 4 (all at 298.15 K); ○, 1 (253.15 K).

data are not tabulated, fitting equations of the form $\log p(H_2O) = A - B/T$ are presented for seven weight percentages of H_2SO_4 (concentrations between 5.22 and 23.79 mol kg^{-1}). In Figure 11 we compare water activities calculated using the present model with values derived from the fitting equations, coupled with the expression for the vapor pressure of pure supercooled water described in footnote b of Table 2. The most notable features of Figure 11 are the very large negative deviations (30–45%) for 23.8 mol kg^{-1} acid, and the positive deviations for 8–22 mol kg^{-1} acid, which occur at all temperatures. Since the present model

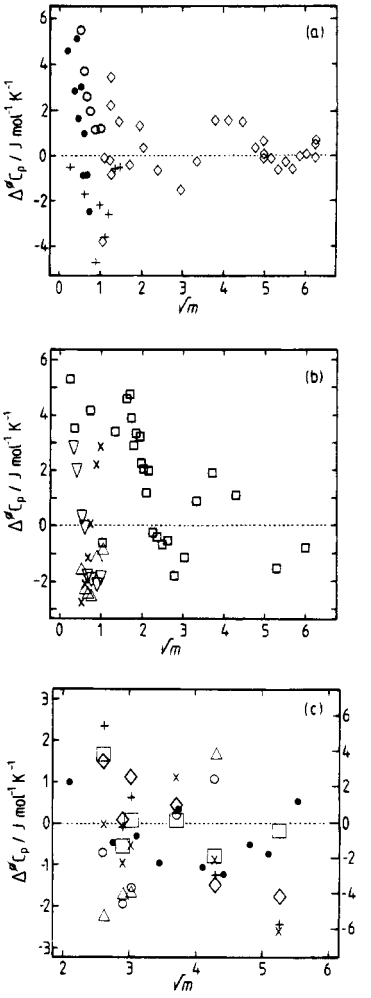

Figure 5. Deviations between measured and fitted apparent molar heat capacities of H_2SO_4. Temperatures (K): (a) 298.15; (b) ×, 328.15; □, 293.15; ▽, 283.15; △, 313.15; (c) ×, 290; +, 280; ◇, 270; □, 260; ●, 253.15; ○, 250; △, 240 (right-hand scale). Sources (N in Table 14): (a) ◇, 1; ●, 2; +, 3; ○, 4; (b) ×, 5; △, 6; □, 7; ▽, 8; (c) ●, 9; other symbols, interpolated using data from sources 10–12 and 14–17 (see text).

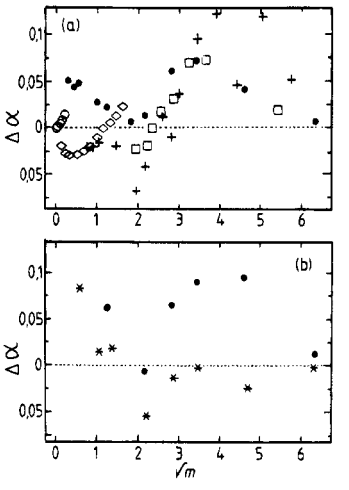

Figure 6. Deviations between measured and fitted degrees of dissociation of the bisulfate ion. Temperatures (K): (a) 298.15; (b) ●, 273.15; *, 323.15. Sources (N in Table 15): (a) ○, 3; ◇, 4; +, 5; ●, 6; □, 7; (b) 6.

represents accurately the large body of thermal data in the region 250 K ≤ T ≤ 273.15 K, together with osmotic coefficients at 273.15 K and emf data to 278.15 K, it is unlikely that it is significantly in error above 250 K.

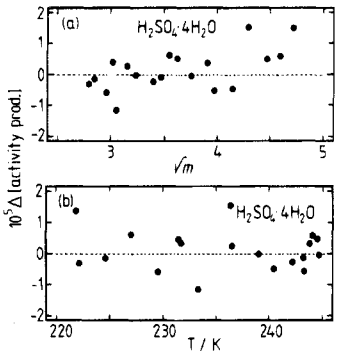

Figure 7. Fitted activity product differences of $H_2SO_4 \cdot 4H_2O$ plotted against (a) $m(H_2SO_4)^{1/2}$ and (b) temperature. The data are from Gable *et al.* (*44*).

Table 6. Activity Products of $H_2SO_4 \cdot nH_2O$ (n = 1, 2, 3, 4, 6.5) in Equilibrium with the Solid Phase Hydrates[a]

solid	a	b	c
$H_2SO_4 \cdot H_2O$	66.922 17	−6434.0498	−0.150 405
$H_2SO_4 \cdot 2H_2O$	0.821 887	−316.5940	
$H_2SO_4 \cdot 3H_2O$	47.453 56	−6758.7767	−0.097 946
$H_2SO_4 \cdot 4H_2O$	68.850 84	-1.014909×10^4	−0.140 118
$H_2SO_4 \cdot 6.5H_2O$	13.107 88	−5167.4839	

[a] Equation: $\ln[a(H^+)^2 a(SO_4^{2-}) a_1^n] = a + b/T + cT$, where T (K) is temperature and activities are on a mole fraction basis. See Table 16 for the temperature ranges over which saturation has been observed, with respect to each of the hydrates, in pure aqueous H_2SO_4.

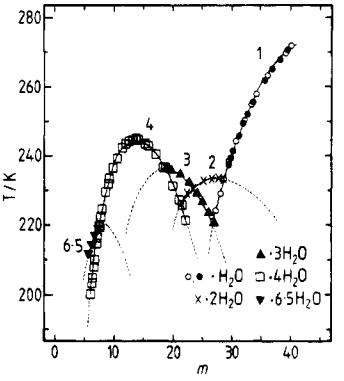

Figure 8. Saturation of pure aqueous sulfuric acid with respect to $H_2SO_4 \cdot nH_2O$, where n = 1, 2, 3, 4, 6.5: symbols, data of Gable *et al.* (*44*) (except filled circles [monohydrate], data of Kunzler and Giauque (*45*)); lines, predicted values using the model, together with equations for the activity products of the hydrates given in Table 6.

Comparison of the work of Zhang *et al.* (*33*) with Zeleznik's results (*5*) at 250 K yields essentially the same pattern of residuals as that shown in Figure 11, as the two models are in substantial agreement for most of the concentrations and temperatures shown. Further calculations of water activity, and hence $p(H_2O)$, for partially frozen mixtures (Figure 4 of Zhang *et al.* (*33*)) also yielded values greater than those measured. At present it is not possible to resolve this discrepancy, and further measurements of water vapor pressure at low temperature would be valuable.

9. Discussion

The mole-fraction-based activity coefficient model used here provides a self-consistent representation of activities and thermal properties of aqueous H_2SO_4 from 0 to 40 mol kg^{-1}, and from 328.15 to below 200 K, within a framework that allows a straightforward extension to solution mixtures. This generality must be balanced against the fact that the model is relatively complex, and contains a large number of interaction parameters. A substantial data set is required for such a model when it is applied over large ranges of temperature and composition—and this is particularly important for aqueous H_2SO_4 which is treated as the mixture $H^+ - HSO_4^- - SO_4^{2-} - H_2O$, where the degree of dissociation of bisulfate cannot be specified *a priori*.

As described in Appendix 2, section c, it was found necessary to constrain the model at very low temperatures using enthalpies calculated from Zeleznik's correlation (*5*) in addition to the experimental data (chiefly saturation with respect to solid phases in this region). Thus, although osmotic coefficients from freezing point measurements (to 201 K), and saturation with respect to $H_2SO_4 \cdot 4H_2O$ (to 220

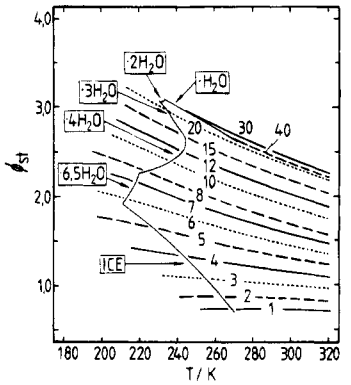

Figure 9. Calculated stoichiometric molal osmotic coefficients for 1.0−40.0 mol kg^{-1} H_2SO_4 as a function of temperature. The number associated with each plotted line is the molality. Freezing points with respect to ice and each of the hydrates are also shown.

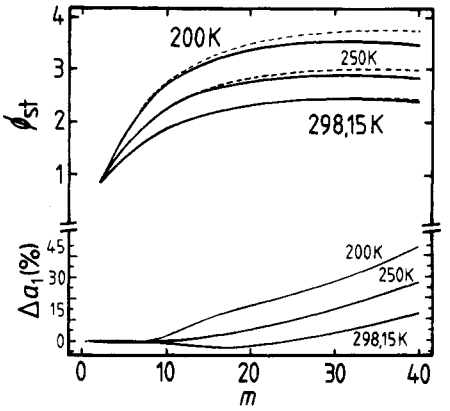

Figure 10. (Top) Stoichiometric osmotic coefficients (ϕ_{st}) calculated using the present model (solid lines) and the correlation of Zeleznik (*5*) (dashed lines). (Bottom) Percentage deviations between the two models in terms of the water activity (a_1).

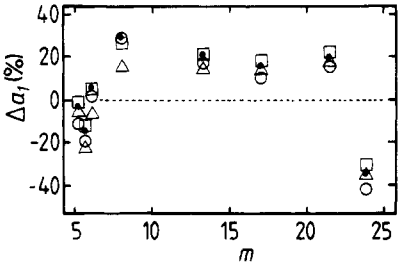

Figure 11. Percentage deviations between water activities calculated using the present model and values derived from the fitting equations of Zhang *et al.* (*33*) together with the expression for the vapor pressure of pure supercooled water described in footnote *b* of Table 2. Temperatures (K): ○, 273.15; ●, 250; □, 235; △, 200.

K), are fitted well by the model, the greatest uncertainties in the treatment occur at low temperature: in the values of ${}^{x}K_{HSO_4}$ (eq 26) and of $C_p(H_2O_{(l)})$ used to calculate ${}^{\phi}C_p$, and the general paucity of data in this region. The effect of the extrapolation of A_x below 273.15 K is not thought important, since at low temperature no solutions exist at high enough dilution for osmotic or activity coefficients to approach the theoretical limiting slopes. The influence of the assumed value of $C_p(H_2O_{(l)})$ on calculated osmotic and activity coefficients at low temperature is difficult to quantify, but probably small, since the apparent molar heat capacity is related only to the second differential of these quantities with respect to temperature. Determination of ${}^{x}K_{HSO_4}$ for $T < 273.15$ K would require measurements of $\Delta_r C_p^\circ$ at these temperatures, which are unlikely to be made for practical reasons. However, the measurement of the degree of dissociation of HSO_4^- at moderate concentrations below 273.15 K, together with activity data, might allow values of ${}^{x}K_{HSO_4}$ to be inferred using the model. Also, further determinations of equilibrium water vapor pressures over aqueous H_2SO_4, at very low temperature, would be of considerable value in verifying the model for practical applications.

Note. The model for aqueous H_2SO_4 described here is available as a FORTRAN77 computer program, available from S.L.C. at the University of East Anglia, or *via* e-mail: S.Clegg@UEA.AC.UK.

Appendix 1

The Debye–Hückel coefficient A_x used here (at 1.0 atm pressure, and as a function of temperature) is equivalent to the molal coefficient obtained by Archer and Wang (*17*), calculated using a program supplied by Archer (personal communication to S.L.C.). Over the temperature range 273.15–373.15 K the Debye–Hückel coefficient is represented by a Chebychev polynomial, whose equation and coefficients are given in Table 8.

The extrapolation of A_x, and enthalpy and heat capacity parameters A_{Hx} and A_{Cx}, to temperatures below 273.15 K must maintain continuity with values at higher temperatures. The three parameters are related by

$$A_{Hx}/RT = 4T(\partial A_x/\partial T)_P \qquad \text{(A1.1)}$$

$$A_{Cx} = (\partial A_{Hx}/\partial T)_P \qquad \text{(A1.2)}$$

The x in the subscript indicates values on a mole fraction basis, but the equations are the same for the molality scale. Because the model is being fitted to heat capacity data, we adopt a linear extrapolation of the heat capacity parameter (A_{Cx}) as the simplest approach:

$$A_{Cx} = A_{Cx}(T_r) + a(T - T_r) \qquad \text{(A1.3)}$$

where $A_{Cx}(T_r)$ is the value of A_{Cx} at the reference temperature T_r (273.15 K). The value of a is set equal to the slope of A_{Cx} with respect to temperature at T_r:

$$a = [(\partial A_{Cx}/\partial T)_P]_{T_r} = 10.864\,511\,27 \qquad \text{(A1.4)}$$

Integrating once with respect to temperature, we obtain

$$A_{Hx} = A_{Hx}(T_r) + A_{Cx}(T_r)(T - T_r) + (a/2)(T - T_r)^2 \qquad \text{(A1.5)}$$

where $A_{Hx}(T_r)$ is the value of A_{Hx} at the reference temperature. Integrating again yields the corresponding expression for A_x:

$$A_x = A_x(T_r) + [A_{Hx}(T_r)/4R](1/T_r - 1/T) + [A_{Cx}(T_r)/4R](\ln(T/T_r) + T_r/T - 1) + (a/8R)(T - T_r^2/T - 2T_r \ln(T/T_r)) \qquad \text{(A1.6)}$$

where $A_x(T_r)$ is the value of A_x at T_r and R is the gas constant (8.3144 J mol^{-1} K^{-1}). Equation A1.6 can also be expressed in the simplified form (eq 30 in the main text)

$$A_x = A + B(1/T_r - 1/T) + C(\ln(T/T_r) + T_r/T - 1) + D(T - T_r^2/T - 2T_r \ln(T/T_r)) \qquad \text{(A1.7)}$$

Values of the various constants in eq A1.6, and equivalent terms in eq A1.7, are given in Table 9. Calculated Debye–Hückel parameters for different temperatures are listed in Table 10.

Appendix 2

The aim of the present study is to provide a self-consistent description of aqueous phase activities and thermal properties of H_2SO_4 from 328 K to very low temperature, and concentrations up to 40 mol kg^{-1}, within a framework that allows ready extension to multicomponent mixtures. The data considered in the previous study of Clegg *et al.* (*6*), using the molality-based Pitzer model, are a subset of those used here.

Measurements cover the period 1899–1990, during which there have been several revisions to both atomic masses and temperature. Changes in atomic masses only affect molality in the fifth significant figure. For consistency we have generally used molar masses of H_2O and H_2SO_4 given by the authors of the various studies; otherwise we have used the following values from the 64th edition of the *CRC Handbook of Chemistry and Physics* (*46*), based upon the 1969 IUPAC recommendations (*47*): H, 1.0079; S, 32.06; O, 15.9994. Conversions of temperature scales to the current ITS-90 are tabulated by Goldberg and Weir (*48*). In general, the δT values applicable to the experimental temperatures are of the same order as the accuracy of temperature control, typically 0.01–0.02 K. Also, the changes in a thermodynamic property (ϕ, emf, etc.) with T are low enough that the change Δ, due to any temperature correction, is small relative to the precision of measurement and the fit of the model. Therefore, where experimental temperatures have been quoted in degrees Celcius they have been converted to absolute values simply by adding 273.15 K.

The different types of thermodynamic data used in this study, and their sources, are discussed briefly below. See Clegg *et al.* (*6*) for further details.

(a) Vapor Pressure and Isopiestic Measurements. Available osmotic coefficients and vapor pressures relevant to the present study are summarized in Table 11. Rard and Platford (*41*) have critically assessed the osmotic coefficients of H_2SO_4 to 27 mol kg^{-1} at 298.15 K. These authors raised serious objections to the use of freezing point depression data to obtain osmotic coefficients (see section f), and circularity regarding the use of $CaCl_2$ as an isopiestic standard in an earlier evaluation (*2*). Because of this—osmotic coefficients of aqueous $CaCl_2$ being largely determined from isopiestic equilibrium with H_2SO_4 solutions—such data are not included here.

Isopiestic data for which aqueous NaCl was the standard have been adjusted to Archer's (*49*) values of ϕ_{NaCl}, as before (*6*). For measurements relative to aqueous KCl the best fit equation of Hamer and Wu (*50*) for ϕ_{KCl}, used by Rard *et al.* (*3*), was also adopted here. The osmotic coefficients of H_2SO_4 for which aqueous NaOH was the standard are

Table 7. Model Calculated Osmotic and Activity Coefficients, Thermal Properties, and Degrees of Dissociation[a]

T/K	$m(H_2SO_4)$	ϕ_{st}	$f_{\pm}^{*'}$	$L(H_2O)$	$L(H_2SO_4)$	$J(H_2O)$	$J(H_2SO_4)$	α
298.15	0.01	0.7867	0.5150	−0.710	14 790	−0.009 79	334	0.554 75
298.15	0.02	0.7438	0.4194	−1.321	17 170	−0.011 6	342	0.446 95
298.15	0.05	0.6982	0.3104	−2.684	19 540	−0.009 90	340	0.330 14
298.15	0.10	0.6751	0.2446	−4.414	20 890	−0.007 83	338	0.268 51
298.15	0.20	0.6642	0.1933	−7.280	22 000	−0.017 1	341	0.231 67
298.15	0.50	0.6756	0.1464	−14.14	23 190	−0.104	355	0.222 37
298.15	0.75	0.6961	0.1332	−19.04	23 630	−0.210	365	0.233 70
298.15	1.00	0.7207	0.1272	−24.43	23 980	−0.330	372	0.247 67
298.15	1.20	0.7426	0.1250	−29.91	24 250	−0.431	377	0.258 84
298.15	1.40	0.7661	0.1245	−37.11	24 560	−0.532	382	0.269 43
298.15	1.60	0.7911	0.1252	−46.62	24 910	−0.627	385	0.279 17
298.15	1.80	0.8173	0.1268	−58.96	25 310	−0.713	388	0.287 95
298.15	2.00	0.8446	0.1293	−74.61	25 770	−0.783	390	0.295 71
298.15	2.50	0.9168	0.1386	−130.6	27 140	−0.866	392	0.310 62
298.15	3.00	0.9930	0.1518	−213.1	28 810	−0.784	391	0.319 44
298.15	3.50	1.071	0.1688	−322.4	30 670	−0.530	386	0.322 88
298.15	4.00	1.150	0.1895	−456.2	32 650	−0.133	380	0.321 82
298.15	4.50	1.228	0.2140	−610.3	34 660	0.356	374	0.317 13
298.15	5.00	1.303	0.2426	−779.7	36 640	0.877	368	0.309 64
298.15	5.50	1.376	0.2752	−960.1	38 550	1.37	363	0.300 10
298.15	6.00	1.446	0.3122	−1 147	40 360	1.80	359	0.289 13
298.15	6.50	1.512	0.3538	−1 339	42 060	2.11	356	0.277 25
298.15	7.00	1.575	0.4000	−1 532	43 650	2.30	354	0.264 88
298.15	7.50	1.634	0.4512	−1 725	45 130	2.36	354	0.252 32
298.15	8.00	1.690	0.5074	−1 917	46 510	2.28	354	0.239 83
298.15	8.50	1.742	0.5690	−2 109	47 800	2.09	356	0.227 58
298.15	9.00	1.791	0.6360	−2 300	49 010	1.77	358	0.215 69
298.15	9.50	1.838	0.7086	−2 490	50 150	1.36	360	0.204 25
298.15	10.00	1.881	0.7871	−2 679	51 220	0.858	363	0.193 30
298.15	10.50	1.921	0.8715	−2 867	52 240	0.282	366	0.182 87
298.15	11.00	1.959	0.9621	−3 055	53 220	−0.356	369	0.172 98
298.15	11.50	1.995	1.059	−3 244	54 150	−1.05	373	0.163 62
298.15	12.00	2.029	1.162	−3 432	55 040	−1.78	376	0.154 78
298.15	12.50	2.060	1.272	−3 621	55 890	−2.55	380	0.146 46
298.15	13.00	2.089	1.388	−3 810	56 720	−3.35	383	0.138 61
298.15	13.50	2.117	1.511	−4 000	57 510	−4.17	387	0.131 24
298.15	14.00	2.142	1.641	−4 191	58 280	−5.01	390	0.124 30
298.15	14.50	2.166	1.777	−4 383	59 030	−5.85	393	0.117 78
298.15	15.00	2.189	1.920	−4 575	59 750	−6.71	397	0.111 66
298.15	15.50	2.210	2.070	−4 769	60 460	−7.57	400	0.105 90
298.15	16.00	2.230	2.227	−4 963	61 140	−8.42	403	0.100 49
298.15	17.00	2.265	2.561	−5 353	62 450	−10.1	408	0.090 63
298.15	18.00	2.296	2.922	−5 746	63 700	−11.8	414	0.081 92
298.15	19.00	2.323	3.310	−6 140	64 880	−13.4	419	0.074 20
298.15	20.00	2.346	3.723	−6 536	66 010	−15.0	423	0.067 36
298.15	21.00	2.365	4.161	−6 932	67 080	−16.5	427	0.061 29
298.15	22.00	2.382	4.623	−7 327	68 100	−18.0	431	0.055 90
298.15	23.00	2.395	5.108	−7 721	69 080	−19.3	434	0.051 09
298.15	24.00	2.406	5.614	−8 113	70 000	−20.6	437	0.046 80
298.15	25.00	2.415	6.140	−8 503	70 890	−21.8	440	0.042 96
298.15	26.00	2.422	6.685	−8 888	71 720	−23.0	443	0.039 53
298.15	27.00	2.427	7.248	−9 270	72 520	−24.0	445	0.036 45
298.15	28.00	2.430	7.826	−9 646	73 280	−25.0	447	0.033 68
298.15	29.00	2.431	8.418	−10 020	74 010	−25.8	448	0.031 19
298.15	30.00	2.431	9.023	−10 380	74 700	−26.7	450	0.028 95
298.15	32.00	2.427	10.27	−11 100	75 970	−28.0	452	0.025 08
298.15	34.00	2.419	11.54	−11 780	77 130	−29.1	454	0.021 90
298.15	36.00	2.408	12.84	−12 440	78 180	−29.9	455	0.019 26
298.15	38.00	2.393	14.15	−13 070	79 120	−30.5	456	0.017 06
298.15	40.00	2.376	15.47	−13 680	79 980	−30.8	457	0.015 22
253.15	*0.01	0.8444	0.6246					0.770 14
253.15	*0.02	0.8020	0.5299					0.683 42
253.15	*0.05	0.7493	0.4097					0.570 22
253.15	*0.10	0.7178	0.3307					0.500 75
253.15	*0.20	0.6972	0.2657					0.456 55
253.15	*0.50	0.6938	0.2031					0.451 35
253.15	*0.75	0.7082	0.1848					0.471 50
253.15	*1.00	0.7305	0.1765					0.493 75
253.15	*1.20	0.7529	0.1739					0.510 55
253.15	*1.40	0.7788	0.1739					0.525 76
253.15	*1.60	0.8079	0.1759					0.539 16
253.15	*1.80	0.8399	0.1796					0.550 66
253.15	*2.00	0.8744	0.1850					0.560 28
253.15	*2.50	0.9698	0.2047					0.576 47
253.15	*3.00	1.075	0.2336					0.582 47
253.15	3.50	1.185	0.2721	−261.3	9 121			0.579 71
253.15	4.00	1.296	0.3212	−401.8	11 200			0.569 57
253.15	4.50	1.406	0.3819	−566.1	13 350			0.553 34

Table 7 (Continued)

T/K	$m(H_2SO_4)$	ϕ_{st}	$f_{\pm}^{*\prime}$	$L(H_2O)$	$L(H_2SO_4)$	α
253.15	5.00	1.512	0.4552	−749.4	15 490	0.532 25
253.15	5.50	1.612	0.5422	−945.8	17 560	0.507 46
253.15	6.00	1.706	0.6438	−1 149	19 530	0.480 11
253.15	6.50	1.793	0.7609	−1 352	21 330	0.451 25
253.15	7.00	1.873	0.8943	−1 552	22 970	0.421 79
253.15	7.50	1.946	1.045	−1 744	24 450	0.392 49
253.15	8.00	2.014	1.214	−1 928	25 760	0.363 97
253.15	8.50	2.076	1.402	−2 103	26 940	0.336 64
253.15	9.00	2.133	1.610	−2 271	28 010	0.310 78
253.15	9.50	2.185	1.840	−2 432	28 980	0.286 55
253.15	10.00	2.234	2.092	−2 589	29 870	0.264 00
253.15	10.50	2.279	2.368	−2 744	30 710	0.243 12
253.15	11.00	2.322	2.669	−2 896	31 500	0.223 87
253.15	11.50	2.361	2.997	−3 048	32 250	0.206 16
253.15	12.00	2.398	3.352	−3 200	32 960	0.189 89
253.15	12.50	2.432	3.736	−3 353	33 660	0.174 97
253.15	13.00	2.464	4.150	−3 507	34 330	0.161 28
253.15	13.50	2.495	4.595	−3 663	34 980	0.148 73
253.15	14.00	2.523	5.072	−3 820	35 620	0.137 21
253.15	14.50	2.550	5.583	−3 979	36 240	0.126 66
253.15	15.00	2.575	6.128	−4 140	36 840	0.116 97
253.15	15.50	2.599	6.708	−4 303	37 440	0.108 07
253.15	16.00	2.621	7.324	−4 468	38 020	0.099 90
253.15	17.00	2.661	8.668	−4 803	39 140	0.085 49
253.15	18.00	2.697	10.16	−5 144	40 230	0.073 31
253.15	19.00	2.728	11.82	−5 491	41 270	0.062 98
253.15	20.00	2.755	13.63	−5 842	42 260	0.054 22
253.15	21.00	2.778	15.60	−6 196	43 220	0.046 77
253.15	22.00	2.798	17.74	−6 552	44 140	0.040 43
253.15	23.00	2.815	20.03	−6 910	45 030	0.035 03
253.15	24.00	2.829	22.48	−7 268	45 870	0.030 43
253.15	25.00	2.841	25.09	−7 624	46 680	0.026 49
253.15	26.00	2.850	27.85	−7 979	47 450	0.023 12
253.15	27.00	2.857	30.75	−8 331	48 190	0.020 24
253.15	28.00	2.862	33.78	−8 679	48 890	0.017 76
253.15	29.00	2.864	36.95	−9 023	49 560	0.015 63
253.15	30.00	2.866	40.23	−9 361	50 200	0.013 79
253.15	32.00	2.863	47.14	−10 020	51 380	0.010 83
253.15	34.00	2.856	54.44	−10 660	52 450	0.008 60
253.15	36.00	2.843	62.05	−11 260	53 410	0.006 91
253.15	38.00	2.827	69.92	−11 840	54 280	0.005 61
253.15	40.00	2.808	77.96	−12 390	55 060	0.004 60
273.15	0.01	0.8253	0.5883	−0.4182	7 417	0.698 54
273.15	0.02	0.7818	0.4917	−0.8670	9 155	0.599 25
273.15	0.05	0.7308	0.3741	−1.966	11 060	0.477 06
273.15	0.10	0.7025	0.2994	−3.341	12 130	0.404 75
273.15	0.20	0.6865	0.2395	−5.262	12 890	0.357 68
273.15	0.50	0.6913	0.1834	−7.652	13 350	0.343 10
273.15	0.75	0.7092	0.1674	−7.922	13 370	0.356 47
273.15	1.00	0.7328	0.1602	−8.562	13 410	0.373 49
273.15	1.20	0.7549	0.1579	−10.45	13 510	0.387 14
273.15	1.40	0.7794	0.1577	−14.41	13 670	0.399 99
273.15	1.60	0.8061	0.1591	−21.12	13 920	0.411 68
273.15	1.80	0.8349	0.1619	−31.22	14 250	0.422 03
273.15	2.00	0.8655	0.1659	−45.22	14 660	0.430 96
273.15	2.50	0.9487	0.1808	−99.87	16 000	0.446 95
273.15	3.00	1.039	0.2023	−185.2	17 720	0.454 27
273.15	3.50	1.132	0.2303	−301.4	19 700	0.453 94
273.15	4.00	1.227	0.2652	−445.5	21 830	0.447 21
273.15	4.50	1.321	0.3074	−612.4	24 010	0.435 41
273.15	5.00	1.411	0.3574	−796.0	26 160	0.419 79
273.15	5.50	1.498	0.4155	−990.2	28 210	0.401 46
273.15	6.00	1.579	0.4824	−1 189	30 130	0.381 42
273.15	6.50	1.656	0.5583	−1 389	31 910	0.360 48
273.15	7.00	1.728	0.6439	−1 586	33 530	0.339 28
273.15	7.50	1.794	0.7396	−1 779	35 010	0.318 30
273.15	8.00	1.856	0.8459	−1 967	36 360	0.297 90
273.15	8.50	1.914	0.9634	−2 150	37 590	0.278 31
273.15	9.00	1.968	1.093	−2 329	38 720	0.259 70
273.15	9.50	2.018	1.234	−2 503	39 770	0.242 13
273.15	10.00	2.064	1.388	−2 675	40 750	0.225 65
273.15	10.50	2.108	1.555	−2 844	41 660	0.210 24
273.15	11.00	2.148	1.736	−3 012	42 530	0.195 88
273.15	11.50	2.186	1.932	−3 179	43 360	0.182 53
273.15	12.00	2.222	2.142	−3 346	44 140	0.170 13
273.15	12.50	2.255	2.368	−3 513	44 900	0.158 63
273.15	13.00	2.286	2.609	−3 681	45 630	0.147 97
273.15	13.50	2.315	2.866	−3 849	46 340	0.138 09

Table 7 (Continued)

T/K	$m(H_2SO_4)$	ϕ_{st}	$f_{\pm}^{*\prime}$	$L(H_2O)$	$L(H_2SO_4)$	α
273.15	14.00	2.343	3.140	−4 018	47 020	0.128 93
273.15	14.50	2.369	3.431	−4 189	47 680	0.120 44
273.15	15.00	2.393	3.738	−4 360	48 330	0.112 57
273.15	15.50	2.415	4.063	−4 533	48 960	0.105 28
273.15	16.00	2.436	4.406	−4 707	49 570	0.098 51
273.15	17.00	2.475	5.145	−5 060	50 760	0.086 41
273.15	18.00	2.508	5.957	−5 417	51 890	0.075 97
273.15	19.00	2.537	6.841	−5 778	52 970	0.066 95
273.15	20.00	2.562	7.798	−6 142	54 010	0.059 15
273.15	21.00	2.584	8.827	−6 510	55 010	0.052 39
273.15	22.00	2.602	9.926	−6 878	55 960	0.046 52
273.15	23.00	2.617	11.09	−7 248	56 870	0.041 41
273.15	24.00	2.6.0	12.33	−7 617	57 740	0.036 96
273.15	25.00	2.640	13.63	−7 986	58 580	0.033 08
273.15	26.00	2.648	14.99	−8 352	59 380	0.029 68
273.15	27.00	2.654	16.40	−8 716	60 140	0.026 70
273.15	28.00	2.658	17.87	−9 077	60 870	0.024 08
273.15	29.00	2.660	19.40	−9 434	61 560	0.021 78
273.15	30.00	2.660	20.96	−9 787	62 230	0.019 75
273.15	32.00	2.657	24.22	−10 480	63 460	0.016 37
273.15	34.00	2.649	27.61	−11 140	64 580	0.013 70
273.15	36.00	2.637	31.11	−11 790	65 600	0.011 58
273.15	38.00	2.622	34.69	−12 400	66 530	0.009 88
273.15	40.00	2.604	38.32	−13 000	67 370	0.008 51
323.15	0.01	0.7406	0.4226	−0.8534	23 550	0.381 94
323.15	0.02	0.7036	0.3359	−1.399	25 690	0.286 20
323.15	0.05	0.6674	0.2430	−2.517	27 640	0.196 70
323.15	0.10	0.6503	0.1889	−3.992	28 780	0.155 73
323.15	0.20	0.6436	0.1476	−6.736	29 840	0.134 62
323.15	0.50	0.6587	0.1103	−14.54	31 170	0.135 56
323.15	0.75	0.6803	0.0998	−21.10	31 760	0.147 70
323.15	1.00	0.7051	0.0949	−28.86	32 250	0.161 29
323.15	1.20	0.7264	0.0930	−36.76	32 650	0.172 06
323.15	1.40	0.7488	0.0922	−46.77	33 080	0.182 39
323.15	1.60	0.7720	0.0923	−59.43	33 550	0.192 10
323.15	1.80	0.7960	0.0931	−75.17	34 060	0.201 13
323.15	2.00	0.8205	0.0944	−94.36	34 620	0.209 45
323.15	2.50	0.8840	0.0997	−159.2	36 220	0.227 11
323.15	3.00	0.9495	0.1073	−249.7	38 040	0.240 50
323.15	3.50	1.016	0.1170	−365.6	40 020	0.250 04
323.15	4.00	1.082	0.1287	−504.0	42 070	0.256 16
323.15	4.50	1.148	0.1424	−660.7	44 110	0.259 30
323.15	5.00	1.212	0.1582	−830.8	46 100	0.259 89
323.15	5.50	1.275	0.1760	−1 010	47 990	0.258 34
323.15	6.00	1.336	0.1961	−1 193	49 770	0.255 02
323.15	6.50	1.394	0.2183	−1 378	51 410	0.250 28
323.15	7.00	1.449	0.2429	−1 563	52 930	0.244 44
323.15	7.50	1.502	0.2698	−1 747	54 340	0.237 76
323.15	8.00	1.553	0.2992	−1 928	55 640	0.230 47
323.15	8.50	1.600	0.3310	−2 108	56 850	0.222 78
323.15	9.00	1.645	0.3654	−2 286	57 980	0.214 84
323.15	9.50	1.687	0.4024	−2 464	59 040	0.206 79
323.15	10.00	1.727	0.4419	−2 641	60 060	0.198 73
323.15	10.50	1.765	0.4841	−2 820	61 020	0.190 75
323.15	11.00	1.800	0.5290	−3 000	61 950	0.182 91
323.15	11.50	1.833	0.5766	−3 182	62 850	0.175 25
323.15	12.00	1.864	0.6268	−3 366	63 720	0.167 81
323.15	12.50	1.893	0.6797	−3 553	64 570	0.160 62
323.15	13.00	1.920	0.7354	−3 742	65 390	0.153 68
323.15	13.50	1.945	0.7937	−3 935	66 200	0.147 02
323.15	14.00	1.969	0.8547	−4 130	66 990	0.140 62
323.15	14.50	1.991	0.9183	−4 329	67 760	0.134 50
323.15	15.00	2.012	0.9846	−4 531	68 520	0.128 64
323.15	15.50	2.031	1.053	−4 735	69 270	0.123 04
323.15	16.00	2.049	1.125	−4 943	70 000	0.117 70
323.15	17.00	2.081	1.275	−5 365	71 420	0.107 74
323.15	18.00	2.109	1.435	−5 797	72 790	0.098 70
323.15	19.00	2.133	1.605	−6 236	74 110	0.090 49
323.15	20.00	2.153	1.783	−6 681	75 370	0.083 04
323.15	21.00	2.171	1.969	−7 131	76 590	0.076 28
323.15	22.00	2.185	2.164	−7 583	77 760	0.070 14
323.15	23.00	2.196	2.365	−8 036	78 880	0.064 56
323.15	24.00	2.206	2.573	−8 489	79 950	0.059 49
323.15	25.00	2.213	2.787	−8 940	80 970	0.054 88
323.15	26.00	2.218	3.007	−9 388	81 940	0.050 68
323.15	27.00	2.222	3.231	−9 832	82 870	0.046 85
323.15	28.00	2.224	3.460	−10 270	83 760	0.043 35
323.15	29.00	2.225	3.692	−10 700	84 600	0.040 16

Table 7 (Continued)

T/K	$m(H_2SO_4)$	ϕ_{st}	$f_{\pm}^{*\prime}$	$L(H_2O)$	$L(H_2SO_4)$	α
323.15	30.00	2.225	3.927	−11 130	85 400	0.037 25
323.15	32.00	2.220	4.406	−11 960	86 890	0.032 13
323.15	34.00	2.212	4.892	−12 750	88 220	0.027 84
323.15	36.00	2.201	5.381	−13 510	89 420	0.024 22
323.15	38.00	2.188	5.870	−14 220	90 490	0.021 15
323.15	40.00	2.172	6.357	−14 900	91 460	0.018 55

[a] Asterisks preceding molalities at 253.15 K indicate solutions supersaturated with respect to ice. Thermal quantities are not tabulated for these solutions. Symbols and units: ϕ_{st} is the stoichiometric molal osmotic coefficient (eq 3); $f_{\pm}^{*\prime}$ is the mean stoichiometric activity coefficient (mole fraction scale) of H_2SO_4 (eq 23); $L(H_2O)$ and $L(H_2SO_4)$ (J mol^{-1}) are the partial molar enthalpies of water and H_2SO_4 in the solution, and $J(H_2O)$ and $J(H_2SO_4)$ (J mol^{-1} K^{-1}) are the relative partial molar heat capacities. Degrees of dissociation α are given to five decimal places so that the free ion activity coefficients of H^+ and SO_4^{2-} can be recovered from $f_{\pm}^{*\prime}$ without loss of accuracy.

Table 8. Chebychev Polynomial Coefficients for Calculating A_x, 273.15 K ≤ T ≤ 373.15 K[a]

a_0	0.826441945	a_6	$-0.885331650 \times 10^{-5}$
a_1	$0.424577529 \times 10^{-1}$	a_7	$0.290299785 \times 10^{-5}$
a_2	$0.415695416 \times 10^{-2}$	a_8	$-0.873435993 \times 10^{-6}$
a_3	$0.687828147 \times 10^{-4}$	a_9	$0.240429892 \times 10^{-6}$
a_4	$-0.358644159 \times 10^{-4}$	a_{10}	$-0.653499789 \times 10^{-7}$
a_5	$0.248305092 \times 10^{-4}$		

[a] The polynomial is represented in Chebychev series form by the normalized variable x [$x = (2X - X_{max} - X_{min})/(X_{max} - X_{min})$], where X is the temperature (K). X_{max} (373.15) and X_{min} (270.15) are the upper and lower limits of the fit, respectively. Note that, for $T \leq 273.15$ K, the empirical extrapolation described in Appendix 1 is employed to calculate values of A_x for use in the model. The polynomial representation of the molality-based Debye–Hückel constant A_ϕ, with 11 ($N + 1$) coefficients, is given by $A_\phi = 0.5a_0T_0(x) + a_1T_1(x) + a_2T_2(x) + a_3T_3(x) + ... + a_NT_N(x)$ where $T_0(x) = 1$, $T_1(x) = x$, and, for $n \geq 2$, $T_n(x) = 2xT_{n-1}(x) - T_{n-2}(x)$. Finally, $A_x = A_\phi(1000/18.0152)^{0.5}$. Values of A_x generated using the polynomial agree with those calculated from the equations of Archer and Wang (*17*) (Archer, personal communication to better than 1 part in 10^5, and the more sensitive heat capacity slope A_{Cx} to ±0.2%. For program validation, the polynomial yields the following values: at 273.15 K, $A_\phi = 0.376\,421\,5$ $mol^{-1/2}$ $kg^{1/2}$; at 298.15 K, $A_\phi = 0.391\,475\,3$ $mol^{-1/2}$ $kg^{1/2}$. Calculated values of A_x, using both this polynomial and the equation given in Appendix 1, are listed in Table 10.

Table 9. Parameters for an Empirical Extrapolation of Debye–Hückel Constants below 273.15 K

parameter[a]	value	parameter[b]	value
$A_x(T_r)$	2.80449621	A	2.80449621
$A_{Hx}(T_r)$	10157.4518	B	305.417462
$A_{Cx}(T_r)$	103.933678	C	3.12511058
a	10.8645113	D	0.163338775

[a] Equation A1.6; T_r is 273.15 K. [b] Equation 29 (main text) and eq A1.7.

based upon Rard *et al.*'s (*3*) evaluation of ϕ_{NaOH} and were taken directly from their Table 1. Water vapor pressures measured by Gordon (*51*), Jones (*52*), and Grollman and Frazer (*53*), and used to determine osmotic coefficients, have been corrected for the nonideality of the vapor phase. The determinations of Hepburn (*54*), as previously noted (*6*), are probably unreliable. Zhang *et al.* (*33*) have recently measured water vapor pressures above aqueous H_2SO_4 (including supercooled solutions) to 200 K. The present analysis was completed before these data became available. However, test calculations suggest that there are inconsistencies, in terms of solvent activity, between the results of Zhang *et al.* (*33*) and both the present model and the correlation of Zeleznik (*5*). These are examined in section 8. For further discussion of both vapor pressure and isopiestic data, see also Rard *et al.* (*3*) and Rard (*40*).

Osmotic coeficient and vapor pressure data at high concentrations are sparse. Therefore, above 16 mol kg^{-1} H_2SO_4, 27 osmotic coefficients calculated from Table 1 of

Table 10. Values of the Debye–Hückel Constant A_x at Different Temperatures[a]

T/K	A_x	T/K	A_x	T/K	A_x
(185.15	1.6621)	(240.15	2.6461)	290.15	2.8781
(190.15	1.8372)	(245.15	2.6769)	295.15	2.9018
(195.15	1.9872)	(250.15	2.7040)	298.15	2.9167
(200.15	2.1154)	(255.15	2.7283)	300.15	2.9268
(205.15	2.2247)	(260.15	2.7507)	305.15	2.9529
(210.15	2.3178)	(265.15	2.7718)	310.15	2.9802
(215.15	2.3968)	(270.15	2.7923)	315.15	3.0087
(220.15	2.4639)	273.15	2.8045	320.15	3.0384
(225.15	2.5209)	275.15	2.8127	325.15	3.0692
(230.15	2.5693)	280.15	2.8336	330.15	3.1013
(235.15	2.6106)	285.15	2.8554		

[a] T is temperature. Values in parentheses are extrapolations given by eq 29 (also eq A1.7); all others are drawn from the evaluation of Archer and Wang (*17*) and reproduced here using the polynomial defined in Table 8.

the evaluation of Giauque *et al.* (*39*) (at 298.15 K) have been included in the model fit. These osmotic coefficients have been given unit relative weight (w_r). The weights assigned to other measurements, and the exclusion of some data sets, are discussed in detail by Clegg *et al.* (*6*), and are given here in Table 11. All data given nonzero weights are shown in Figure 12.

(b) EMF Measurements. Sources of electromotive force data are listed in Table 12 for the following electrochemical cells:

$$(Pt)\ H_2\ |H_2SO_4(m)|PbSO_4,\ PbO_2\ (Pt) \qquad (I)$$

$$E = E^\circ + (RT/(2F))\ \ln(m(H^+)^2\gamma_H{}^2 m(SO_4{}^{2-})\gamma_{SO_4}/a_1{}^2) \qquad (A2.1)$$

$$(Pt)\ H_2|H_2SO_4(m)|Hg_2SO_4,\ Hg\ (Pt) \qquad (II)$$

$$E = E^\circ - (RT/(2F))\ \ln(m(H^+)^2\gamma_H{}^2 m(SO_4{}^{2-})\gamma_{SO_4}) \qquad (A2.2)$$

$$Hg,\ Hg_2SO_4|H_2SO_4(m)|PbSO_4,\ PbO_2\ (Pt) \qquad (III)$$

$$E = E^\circ + (RT/F)\ \ln(m(H^+)^2\gamma_H{}^2 m(SO_4{}^{2-})\gamma_{SO_4}/a_1) \qquad (A2.3)$$

$$Pb–Hg(amalgam),\ PbSO_4|H_2SO_4(m)|H_2\ (Pt) \qquad (IV)$$

$$E = E^\circ + (RT/(2F))\ \ln(m(H^+)^2\gamma_H{}^2 m(SO_4{}^{2-})\gamma_{SO_4}) \qquad (A2.4)$$

where E and E° are, respectively, the measured and standard emfs (V) of the cells, R (8.3144 J mol^{-1} K^{-1}) is the gas constant, and F (96484.6 C mol^{-1}) is Faraday's constant. In the above equations, concentrations and activity coefficients are expressed on a molality basis.

Table 11. Availability of Isopiestic and Vapor Pressure Data for Aqueous H_2SO_4[a]

$m(H_2SO_4)$	T/K	no. obsd[b]	method	std	rel wt	no. rejected[b]	N	ref
1.673–21.65	298	33	iso	NaOH	1.0	29	1	74
2.083–4.354	298	12	iso	NaCl	1.0	0	2	75
0.019–4.349	298	18	iso	NaCl	0.25	3	3	76
0.091–2.830	298	23	iso	KCl	0.25/0.75[c]	1	4	77
0.091–4.374	298	28	iso	NaCl	0.25/0.75[c]	2	5	77
0.195–3.136	298	53	iso	KCl	0.25	0	6	78
1.918–22.63	298	20	vp		1.0	1	7	51
0.073–2.871	298	13	vp		1.0	9	8	53
13.88–27.74	298	3	vp		1.0	0	9	79
7.326–12.58	298	9	vp			9	10	54
0.346–4.361	298	44	iso	NaCl	1.0	0	11	40
4.349–19.33	298–409	146	vp		0.1	*d*	12	80
1.133–40.78	298[e]	12	vp		0.1	8	13	52
2.091–4.355	298	16	iso	NaCl	1.0	0	14	81
0.141–0.170	298	4	iso	KCl	1.0	0	15	82
0.442–0.487	298	3	iso	KCl	1.0	0	16	*f*
0.189–4.175	323	44	iso	NaCl	1.0	5	17	*g*
1.450–4.096	273	8	iso	NaCl	0.25	2	18	83
1.033	273	1	iso	urea	0.25	0	19	83
1.14–9.56	273–373	99	vp			99	20	84
20–65	298	44 (26)[h]	iso	H_2SO_4		26	21	85
1.00 *to* >100 wt %	298	126 (67)[i]	vp		1.0	0	22	39
4.026–4.420	298	4	iso	NaCl	1.0	0	23	*j*
5.217–23.79[k]	203–250	*l*	vp				24	33

[a] N is the data set number, referred to in the figures. Osmotic coefficients relative to the NaCl isopiestic standard were calculated using eq 7 and eq 36 of Archer (*49*). (Note that Clegg *et al.* (*6*) give corrections to Archer's eq 36.) [b] The second number in parentheses gives the number of data points within the fitted concentration range 0–40.9 mol kg^{-1}; the number in the no. rejected column refers only to those points within the fitted range. Molalities of the rejected data for each reference: 1.673–4.376, 5.002, 5.144, 8.744–21.65 (*74*); 0.0187, 0.0456, 3.815 (*76*); 0.0909, 0.0908, 4.374 (77); 2.239 (*51*); 0.073–1.282, 2.468 (*53*); 3.399, 5.490, 10.196–23.791 (*80*); 1.133–6.797, 12.462, 15.294, 30.587, 40.782 (*52*); 0.3037, 0.2576, 0.1894, 2.1157, 3.1911 (g); 1.450, 2.186 (*83*); 1.133–6.797, 12.462, 15.294, 30.587, 40.782 (*52*). [c] Concentrations below 1.0 mol kg^{-1} are given the lower weight of 0.25. [d] Concentration and temperature ranges are those of the experimental determinations. Only 12 values (7 of which were rejected) were used here, taken from the interpolated 25 °C isotherm in Collins' Table 3 (*80*). [e] Data for some other temperatures given graphically. [f] J. A. Rard, work in progress. [g] D. A. Palmer and F. H. Sweeton, personal communication. [h] Numbers in this column refer to tabulated ϕ_{st} at round concentrations, as original experimental data are not given. A bithermal isopiestic technique was used, with the H_2SO_4 standard at 4 °C. [i] Giauque *et al.* tabulate $F_1^\circ - F_1$, calculated from vapor pressure and other data. This quantity is related to water activity (a_1) by the equation $(F_1 - F_2)/RT = \ln(a_1)$. Because many data are available at low concentrations, only 27 values ($m(H_2SO_4) > 16$ mol kg^{-1}) were used here. [j] J. A. Rard and D. G. Archer, unpublished data. [k] Vapor pressures also measured along the freezing curve of sulfuric acid tetrahydrate and hemihexahydrate. [l] Representative data presented only in graphical form, and also as fitting equations. The measurements of Zhang *et al.* (*33*) were not included in the present treatment, but are compared with model predictions and also with the work of Zeleznik (*5*) (section 8).

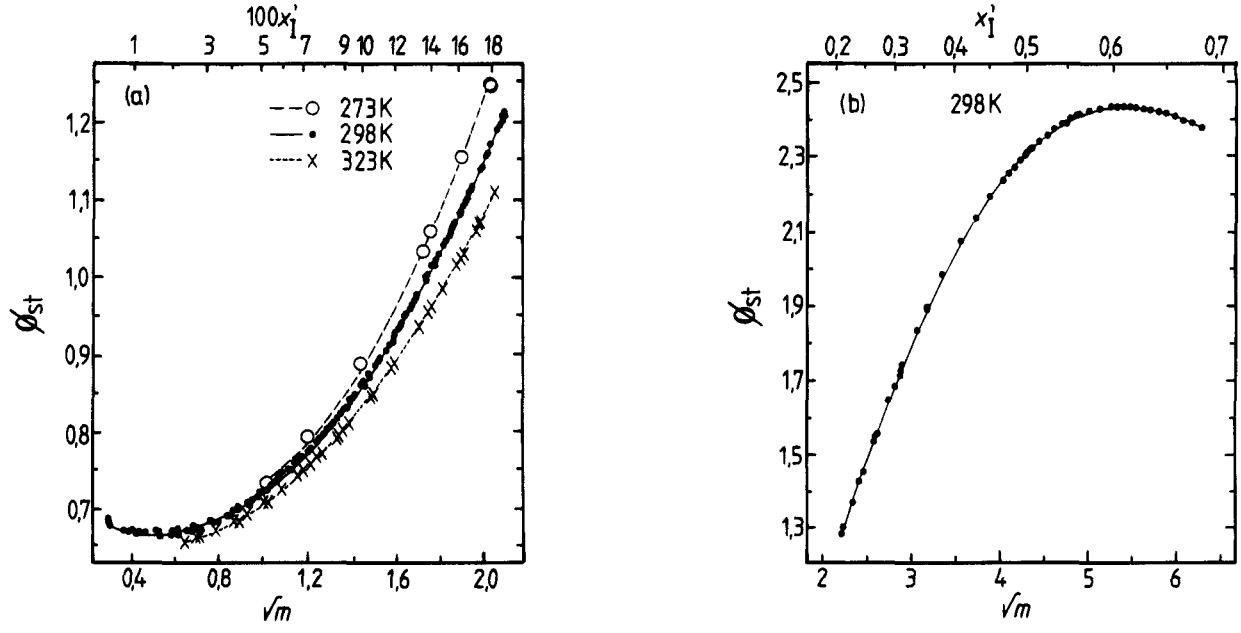

Figure 12. Stoichiometric osmotic coefficient (ϕ_{st}) of aqueous H_2SO_4 at three temperatures plotted against $m(H_2SO_4)^{1/2}$ and the stoichiometric total mole fraction of ions, x_I' (eq 21). See Table 11 for a list of the individual data sets. The solid and dashed lines are the fitted model.

During the fitting of the model these quantities were calculated from their mole fraction equivalents, so that eqs A2.1–A2.4 could be used directly. As in the previous study (*6*), we do not consider emf measurements involving electrolyte mixtures HCl–H_2SO_4–H_2O (*55*, *56*) or $NaHSO_4$–Na_2SO_4 (*22*), nor the early work of Hamer (*57*) and Harned and Hamer (*58*) which has been shown by several authors to be inconsistent with modern data (*59–61*).

Table 12. Availability of emf Data for Cells I–IV[a]

cell	$m(H_2SO_4)$	T/K	no. obsd[b]	intl[c]	rel wt	no. rejected[b]	N	ref
I	0.1000–8.272	278–328	77	yes	1.0	0	1	60
I	0.0073–0.096	298	5	no	1.0	0	2	59
I	0.0195–0.997[d]	298	19	yes		19	3	57
II	0.0050–0.050	298	2	yes		2	4	86
II	0.1003–7.972	278–328	54	no	1.0	7	5	61
II	0.0073–0.096	298	13	no	1.0[e]	0	6	59
II	0.0506–2.386	298	7	yes	1.0	0	7	87
II	0.0506–8.207	298	5	yes	1.0	1	8	88
II	0.0010–0.010	298	5	no		5	9	89
II	0.0050–1.041	298	6	yes	1.0[e]	2	10	90
II	0.1000–4.000	298	7	yes	1.0	2	11	91
III	0.0536–3.499	298	10	yes	1.0	2	12	92
IV	0.0010–0.020	273–323	25	yes	1.0	12	13	93

[a] N is the data set number, referred to in the figures. Absolute temperatures given by Covington *et al.* (*59*) and Beck *et al.* (*60*, *61*) are based upon an ice point of 273.16 K = 0 °C (*94*). We have therefore subtracted 0.01 K from the temperatures given by these authors. Values of the coefficients for eq A2.5, giving the standard potentials of each cell over the specified temperature ranges, are as follows:

cell	T	r_1	r_2	r_3
I	278.15–328.15	1.690 998	8.883 153	0.202 140 7
II	278.15–328.15	0.612 357 3	−7.273 884	−0.248 245 9
III	298.15	1.077 553		
IV	273.15–323.15	0.352 767 9	6.844 644	0.266 346 36

[b] Molalities of the rejected data for each reference: 1.872, 5.767 (278 K); 0.1003, 1.872 (318 K); 0.1003, 1.872, 5.767 (328 K) (*61*); 8.207 (*88*); 0.02506, 0.2529 (*90*); 2.0, 4.0 (*91*); 0.5154, 1.036 (*92*); 0.001 and 0.002 (all temperatures); 0.005, 0.02 (273 K) (*93*). [c] The change from international to absolute volts [1.0 V (intl) = 1.000 33 V (abs)] occurred in 1948. Results published after this year are assumed to be in absolute volts, except for the work of Beck *et al.* (*60*) (A. K. Covington, personal communication). [d] Measured values (Hamer's Table I) using the preferred methods (4–6) of electrode preparation. [e] For concentrations <0.04 mol kg^{-1} H_2SO_4, relative weights were reduced to 0.5 as the model-calculated emf is sensitive to the amount of Hg_2SO_4 assumed to be present (see text).

For measurements at low molalities of H_2SO_4, dissolved $PbSO_4$ and Hg_2SO_4 can contribute significantly to the total concentration of the solution. The presence of the soluble sulfates in the cells is accounted for within the model by an increase in total ionic strength I_x (assuming both salts to be fully dissociated) and sulfate mole fraction $x(SO_4^{2-})$.

Equilibrium concentrations of $PbSO_4$, calculated from the tabulation of Shrawder and Cowperthwaite (*93*) are assumed to be present in the solutions in cells I, III, and IV. For $m(H_2SO_4) > 0.02$ mol kg^{-1} the dissolved $PbSO_4$ concentration is low enough (<0.022 × 10^{-3} mol dm^{-3}) to be neglected. As the $PbSO_4$, Pb electrode may only be reliable for $m(H_2SO_4) > 0.005$ mol kg^{-1} (*27*), measurements for cell IV below this molality have been discarded. Concentrations of the more soluble mercurous sulfate have been estimated by interpolation from the data of Craig *et al.* (*62*). As before (*6*), in view of the very simple treatment of the effect of the dissolved salt, and its relatively high solubility, data weights for $m(H_2SO_4) < 0.04$ mol kg^{-1} (cell II) were reduced to 0.5.

For cells I and II there are two and six data sets, respectively, at 298.15 K. It is possible for systematic deviations in $E°$ (bias potentials) to occur for different electrode preparations of the same type. This question has been addressed previously (*6*), and the values of the bias potentials that were estimated have been included here, as adjustments ($\Delta E°$) to the standard potentials for particular data sets. The standard potentials themselves are also fixed to the values determined by Clegg *et al.* (*6*), given by the general equation

$$E° = r_1 + 10r_2(1/T - 1/T_r) + 10^{-3}r_3(T\ln(T) - T_r\ln(T_r)) \quad \text{(A2.5)}$$

where T (K) is the temperature, T_r is the reference temperature of 298.15 K, and the coefficients r_{1-3} are listed in Table 12.

With the exception of the low-concentration data for cell II mentioned above, all retained emf measurements have been given unit relative weight. See Clegg *et al.* (*6*) for plots of the data.

(c) Apparent Molar Enthalpies. Sources of enthalpy data (differential heats of dilution) are listed in Table 13. Experimental dilutions ($m_1 \rightarrow m_2$) are about 30% for the work of Kunzler and Giauque (*63*), 10% or less for the determinations of Wu and Young (*64*) and most of Groenier's work (*65*), and greater than 90% for the results of Lange *et al.* (*66*) and three experiments of Groenier. The most precise data are those of Wu and Young (*64*), who have also calculated $^{\phi}L$ from their own work and that of the other authors given above. Clegg *et al.* (*6*) have evaluated the 0–6 mol kg^{-1} data at 298.15 K, and the exclusions and relative weights assigned in that study have been adopted here without alteration. Generally, points with a deviation of >40 J mol^{-1} were rejected, and the relative weights (w_r) given in Table 13 were derived as $1/\sigma^2$, compared to Wu and Young's (*64*) tabulated $^{\phi}L$.

In this study we are also able to include heats of dilution measured by Kunzler and Giauque (*63*) at 253.15 K. Comparisons with model calculations suggested that the precision was slightly less than Kunzler and Giauque were able to achieve at 298.15 K, but the measurements were assigned a unit relative weight as they constitute the only low-temperature data set.

Data given nonzero weights are plotted in Figure 13 as $\delta^{\phi}L/\delta m^{1/2}$, corrected for the difference between this quantity and the measured $-\Delta_{dil}H/(m_1^{1/2} - m_2^{1/2})$. This correction,

Table 13. Availability of Enthalpy Data (Heats of Dilution) for Aqueous H_2SO_4[a]

$m(H_2SO_4)$[b]	T/K	no. obsd[c]	rel wt	no. rejected[c]	N	ref
(>100 wt %)–0.506[d]	298	72 (26)	1.0	4	1	63
6.423–0.001	298	25	2.23	0	2	64
3.679–0.003	298	45	0.86	7	3	65
0.050–0.003[e]	298	11	0.045	6	4	66
30.860–6.07[f]	253	10	1.0	0	5	63
0.005–6.0[g]	303–598				6	95

[a] N is the data set number, referred to in the figures. Also included in the fit are 168 partial molar enthalpies of water ($L(H_2O)$) from 2 to 40 mol kg^{-1} and from 185.15 to 245.15 K generated from equations given by Zeleznik (*5*). These were introduced in order to constrain the model at very low temperatures, and did not significantly affect the fit to the experimental enthalpy and heat capacity data (which were themselves included in Zeleznik's correlation). [b] Range given for initial molality m_1. [c] The second number in parentheses gives the number of data points within the fitted concentration range 0–40.9 mol kg^{-1}; the number in the no. rejected column refers only to those points within the fitted range. Molalities (m_1) of the rejected data for each reference: 1.508, 1.040, 0.726, 0.506 (*63*); 0.0251 (two points), 0.0125, 0.006 27, 0.003 13 (two points) (*66*); 0.003 05, 0.005 04, 0.005 08, 0.0174 (three points), 0.0846 (*65*). [d] See also corrections given by Giauque *et al.* (*39*). Differential heats of dilution were calculated as $\Delta_{dil}H = {}^{\phi}L_2 - {}^{\phi}L_1 = (\Delta A)L_1$ (Table 3 of Kunzler and Giauque (*63*)). [e] Mol dm^{-3} concentrations converted to molality using densities compiled by Söhnel and Novotný (*96*). [f] The tabulated L_1 are based upon $H_1° = 0$ at 298.15 K, and were adjusted by adding 820.86 cal mol^{-1}. [g] Experiments were carried out at 7–40 MPa, and are therefore not relevant to the present study.

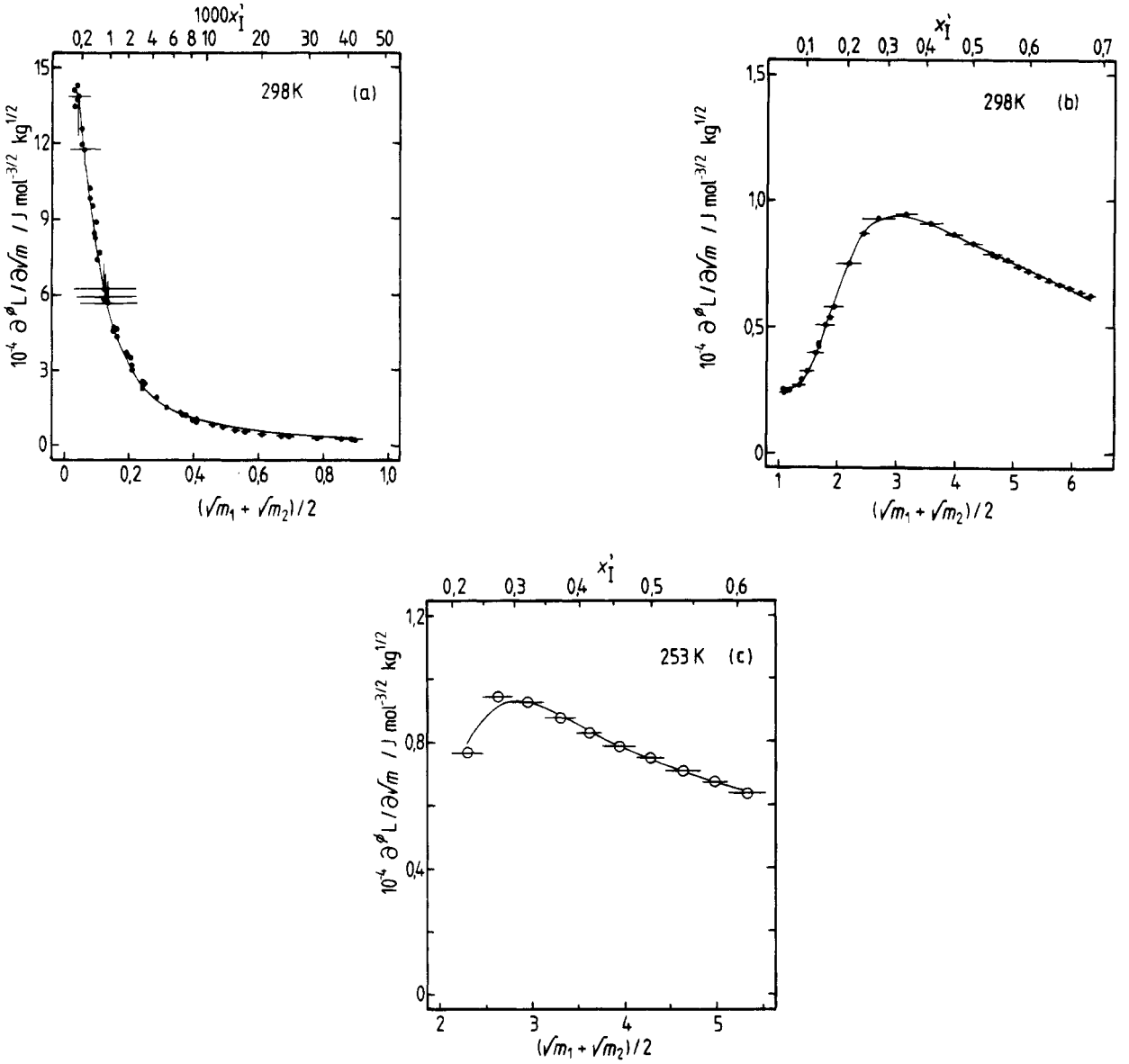

Figure 13. Differential of the apparent molal enthalpy with respect to $m(H_2SO_4)^{1/2}$, $(\partial^{\phi}L/\partial m^{1/2})$, calculated from heats of dilution at 298.15 and 253.15 K, and plotted against the mean of the initial and final molalities and the corresponding x_I'. Horizontal lines indicate the extent of the dilution $m_1 \rightarrow m_2$. Vertical lines indicate the correction from $-\Delta_{dil}H/[(m_1^{1/2} + m_2^{1/2})/2]$ to the true differential as plotted, which was estimated from the tabulated $^{\phi}L$ of Wu and Young (*64*) (for $m(H_2SO_4) < 6$ mol kg^{-1}) and with the model at higher concentrations. In most instances this correction is too small to be shown. See Table 13 for the sources of the experimental measurements. The lines represent the fitted model.

significant only for the results of Lange *et al.* (*66*), is also shown as is the range of dilution $(m_1^{1/2} - m_2^{1/2})$. Note that the data were fitted directly as $\Delta_{dil}H$.

In order to constrain the model better at very low temperature, we have included in the fit partial molar enthalpies of water ($L(H_2O)$, J mol^{-1}) from the evaluation of Zeleznik (*5*) (see footnotes to Table 13). Initial model results (with $L(H_2O)$ excluded from the data set) showed good agreement with Zeleznik's values for $m(H_2SO_4) \leq 10$ mol kg^{-1} down to 240 K. At higher molalities, over the same range of temperature, values differed by almost constant amounts at each molality. This is unsurprising, given that the two models yield different water activities, at high concentration, even at 298.15 K. The partial molar enthalpies of Zeleznik were therefore fitted directly for $m(H_2SO_4) \leq 10$ mol kg^{-1}, and with single $\Delta L(H_2O)$ terms (adjustable by the model) at each higher molality.

(d) Apparent Molar Heat Capacities. Heat capacity measurements for H_2SO_4–H_2O are summarized in Table 14. For completeness we have included all the data of Giauque and co-workers even though some determinations are outside the concentration range of the present study. Abel (*67*) considers that, of measurements made prior to about 1945, only the data of Biron (*68*) and to a lesser extent Savarizky (tabulated by Socolik (*69*)) are reliable. Biron's work has been used by Craig and Vinal (*70*) in their study of aqueous H_2SO_4 related to the lead storage battery, and that of Savarizky by Giauque *et al.* (*39*) to estimate temperature coefficients of partial molar properties. Here, as before (*6*), we have not used the work of Savarizky. Details of the calculation of apparent molar heat capacities from measured specific heats ($T > 273.15$ K), and the adjustment of the data of Randall and Taylor (*71*), are given by Clegg *et al.* (*6*). Because of the extended range of the present model application, it is possible to include heat capacities below 273.15 K. These have been measured by Kunzler and Giauque (*63*) at a fixed temperature of 253.15 K, and for various concentrations as a function of temperature; see Table 14. As stated previously, heat capacities of pure water below 273.15 K were extrapolated from Hill's

Table 14. Availability of Enthalpy Data (Heat Capacities) for Aqueous H_2SO_4[a]

$m(H_2SO_4)$	T/K	no. obsd[b]	rel wt	no. rejected[b]	N	ref
1.149–(>100 wt %)[c]	298	75 (32)	1.0	2	1	63
0.052–0.563	298	9	1.0	0	2	97
0.044–2.230[d]	298	13	1.0	4	3	71
0.103–1.013	298	8	0.50	2	4	29
0.103–1.013	328	8	0.50	2	5	29
0.103–1.013	313	8	0.50	2	6	29
0.035–(100 wt %)	293	37 (29)	0.25	1	7	68
0.103–1.013	283	8	0.50	0	8	29
4.508–30.898	253	11	1.0	0	9	63
9.2468	214–300	11	1.0	e	10	98
8.5385	230–319	14	1.0	e	11	98
6.9377	213–296	11	1.0	e	12	98
55.509	284–305	4 (0)		e	13	99
27.754	239–306	12	1.0	e	14	99
18.503	182–298[f]	12	1.0	e	15	100
18.503	244–296[f]	8	1.0	e	16	101
13.881	251–305	9	1.0	e	17	101

[a] N is the data set number, referred to in the figures. Socolik (*69*) tabulates specific heats (to three figures) of Savarizky (unreferenced) at 22.5, 40, 60, and 80 °C from 6.06 to 100 wt % H_2SO_4. [b] The second number in parentheses gives the number of data points within the fitted concentration range 0–40.9 mol kg^{-1}; the number in the no. rejected column refers only to those points within the fitted range. Molalities of the rejected data for each reference; 1.586, 1.231 (*63*); 0.0444, 0.0713, 0.1748, 0.5515 (*71*); 0.1035, 0.1781 ($T \geq 298.15$ K) (*29*); 0.0347 (*68*). [c] See also corrections given by Giauque *et al.* (*39*). [d] These heat capacities are on a per gram of H_2O basis. This is not stated in the paper, and caused Zeleznik (*5*) to reject their results as erroneous. [e] See text for explanation of how these data were incorporated. [f] Includes supercooled solutions.

equation of state (*34*) using the value of $C_p(H_2O_{(l)})$ at 273.15 K together with first and second differentials with respect to temperature. These yield the following equation:

$$C_p(H_2O_{(l)}) = 75.9938 - 0.064242(T - 273.15) + 2.7023 \times 10^{-3}(T - 273.15)^2 \quad \text{(A2.6)}$$

where $C_p(H_2O_{(l)})$ is in J mol^{-1} K^{-1} and T (K) is temperature. Apparent molar heat capacities ($^{\phi}C_p$) were calculated from the data of Kunzler and Giauque (*63*) using $C_p(H_2O_{(l)})$ given by eq A2.6 below 273.15 K, and by the *CRC Handbook of Chemistry and Physics* (*46*) at higher temperatures. Values of $^{\phi}C_p$ were then interpolated for each concentration at 10 K intervals from 240 to 290 K.

Test applications of the model, where $^{\phi}C_p$ values below 273.15 K were included, showed good consistency with other data at higher temperatures. Relative weights of 1.0 were therefore assigned, with the exception of values at 240 K where w_r was reduced to 0.1. Relative weights for other data sets are as given by Clegg *et al.* (*6*), and listed here in Table 14.

The infinite dilution value of the apparent molar heat capacity ($^{\phi}C_p^{\circ}$, J mol^{-1} K^{-1}), which varies as a function of temperature, has been fixed to values determined by Clegg *et al.* (*6*) over the temperature range 283.15–328.15 K, and is given by the equation

$$^{\phi}C_p^{\circ} = -286.175 + 3.677433(T - 298.15) - 0.04710391(T - 298.15)^2 \quad \text{(A2.7)}$$

The value of $^{\phi}C_p^{\circ}$ can also be obtained from data for other compounds, since the apparent molar properties of ions are additive. Gardner *et al.* (*72*) have done this, using integral heats of solution. Their tabulated $^{\phi}C_p^{\circ}$ (from 273 to 373 K) agree with eq A2.7 to within 33 J mol^{-1} K^{-1} from 283.15 to 323.15 K.

Values of $^{\phi}C_p^{\circ}$ for $T < 283.15$ K have been fitted by the model as unknowns. It is probably unwise to attach particular thermodynamic significance to these estimates, since they are necessarily dependent upon, first, the value of $^{x}K_{HSO_4}$ used (and its temperature dependence) which are uncertain at low temperature, second, the model extrapolation to infinite dilution, and third, the assumed value of $C_p(H_2O_{(l)})$ below 273.15 K. All data given nonzero weights are plotted in Figure 14.

(e) Degree of Dissociation of the Bisulfate Ion. Studies of the degree of dissociation, α, are listed in Table 15. We have found that even where the model is fitted simultaneously to activity, osmotic coefficient, and thermal data the speciation is not fully constrained—particularly its variation with temperature; thus, it is worthwhile to include measurements of α in the fit. Considering the

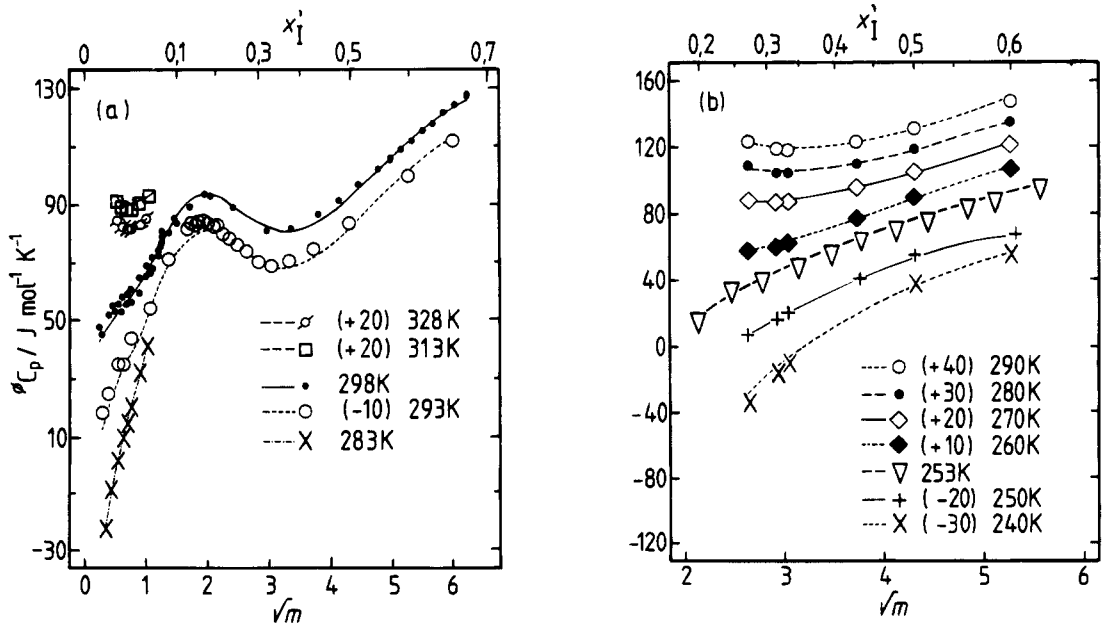

Figure 14. Apparent molar heat capacities ($^{\phi}C_p$) of H_2SO_4 at different temperatures (indicated on the graph) plotted against $m(H_2SO_4)^{1/2}$ and x_I'. For clarity, data at all temperatures except 298.15 and 253.15 K are offset vertically by fixed amounts indicated in parentheses on the graphs. The lines represent the fitted model. See Table 14 for the sources of the experimental measurements.

Table 15. Availability of Degree of Dissociation Data ($HSO_4^- \rightleftharpoons SO_4^{2-} + H^+$) for Aqueous H_2SO_4[a]

$m(H_2SO_4)$	method[b]	T/K	no. obsd[c]	rel wt	no. rejected[c]	N	ref
0.01–0.304	1	300	10		10	1	102
0.02–4.00[d]	2	298	10		10	2	103
0.00025–0.050	3	298	7	1.0	0	3	104
0.00090–2.634	4	298	13	1.0	0	4	105
0.264–42.62	2	298	18 (17)	1.0	3	5	106
0.050–40.15[e]	2	273–323	28	1.0	2	6	16
0.52–29.26[e]	5	298	12	1.0	2	7	73

[a] N is the data set number, referred to in the figures. References above are restricted to studies of the variation of α as a function of concentration, and do not include those whose sole aim is to determine the infinite dilution value of K_{HSO_4}. Kerker (*107*) recalculated α from literature data (including those of Sherrill and Noyes (*104*)), but many values are grossly discordant with other work, and have not been used. [b] Methods: 1, spectrophotometry; 2, Raman spectroscopy; 3, conductance; 4, molar volume; 5, nuclear magnetic resonance. [c] The second number in parentheses gives the number of data points within the fitted concentration range 0–40.9 mol kg^{-1}; the number in the no. rejected column refers only to those points within the fitted range. Molalities of the rejected data for each reference: 0.52, 1.03 (*73*); 2.915, 1.377, 0.264 (*106*); 0.502, 0.504 (*16*). [d] Concentrations in mol dm^{-3}. [e] Data also available for the first dissociation ($H_2SO_4 \rightleftharpoons H^+ + HSO_4^-$).

Table 16. Availability of Data for Equilibrium with Solid Phases[a]

solid	T/K	mol % H_2SO_4	no. obsd	used[b]	rel wt	no. rejected[b]	ref
H_2O[c]	272.6–201.9	0.34–9.78	21	yes	1.0/0.5[d]	2	44
$H_2SO_4 \cdot 4H_2O$	200.1–244.8	9.94–28.61	32	yes	1.0	*e*	44
$H_2SO_4 \cdot 6.5H_2O$[f]	219.4–211.2	9.28–11.92	6				44
$H_2SO_4 \cdot 3H_2O$	236.6–220.3	25.18–32.52	9				44
$H_2O_4 \cdot 2H_2O$	225.7–233.3	27.90–33.97	9				44
$H_2SO_4 \cdot H_2O$	221.0–281.7	32.52–73.46	36				44
H_2SO_4	238.3–283.5	73.46 to >100	28				44
$H_2SO_4 \cdot H_2O$	237.5–281.7	34.7–72.2	61				45
H_2SO_4	239.5–283.5	73.6 to >100	51				45

[a] Gable *et al.* (*44*) have also determined equilibrium with respect to $H_2S_2O_7$. [b] See text for details of how these data were incorporated into the present model. The first two (lowest) molalities for the ice solid phase were not used. [c] Many freezing point depression measurements (at low H_2SO_4 concentrations) are also available. However, these are considered to be in error (*6*) and are not listed here. See also Rard and Platford (*41*). [d] Three data points at high molality (5.361, 5.953, and 6.0188 mol kg^{-1}) were given a reduced weight. [e] Only data from the temperature range for which two liquid compositions are simultaneously in equilibrium with the solid phase are used (see text). Hornung *et al.* (*98*) suggest that the ice + tetrahydrate eutectic point listed by Gable *et al.* (*44*) is ice + octahydrate. [f] Given by Gable *et al.* (*44*) as $H_2SO_4 \cdot 6H_2O$, but shown by Hornung *et al.* (*98*) to be the hemihexahydrate.

different methods used, agreement between the data sets is quite good. At 298.15 K, α decreases rapidly from 100% at infinite dilution to about 20% at 0.4–0.5 mol kg^{-1}, thereafter rising to a broad peak of ~30% from 2 to 6 mol kg^{-1} and then decreasing slowly.

Speciation determined from nuclear magnetic resonance (NMR) and Raman spectral data are least reliable for dilute solutions, and values for $m(H_2SO_4) < 2$ mol kg^{-1} of Hood and Reilly (*73*) have been discarded. At temperatures other than 298.15 K there are only the data of Young *et al.* (*16*). One point at 273.15 K (0.504 mol kg^{-1}) was discarded, and on the basis of tests of consistency with other thermodynamic data (using the model), all measurements were assigned unit relative weight.

All data given nonzero weights are plotted in Figure 15.

(f) Freezing Point Depression. Measurements of the freezing temperatures of solutions yield the osmotic coefficient of the solution at the freezing temperature, as discussed in section 4. The many different studies are listed by Staples (*2*) and by Clegg *et al.* (*6*). After comparisons with measured ϕ_{st} at 298.15 K and thermal data, Clegg *et al.* (*6*) concluded that, at least below 0.1 mol kg^{-1}, the data were systematically in error. Rard (*40*) and Rard and Platford (*41*) came to a similar conclusion, suggesting that the precipitating solid phase could well be dilute H_2SO_4 rather than pure ice. Clegg *et al.* therefore did not use freezing point depression data in their model. However, given our particular interest in low-temperature properties and the importance of the precipitation of solid phases in real systems, freezing point data for the precipation of ice (0.58–6.02 mol kg^{-1} H_2SO_4) and of $H_2SO_4 \cdot 4H_2O$ (7.85–22.2 mol kg^{-1} H_2SO_4) are included here; see Table 16. The calculation of stoichiometric osmotic

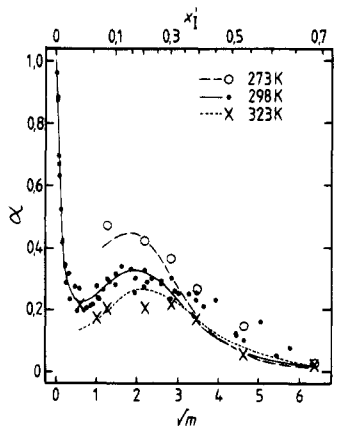

Figure 15. Degrees of dissociation (α) of the bisulfate ion, at different temperatures, plotted against $m(H_2SO_4)^{1/2}$ and x_1'. The lines represent the fitted model. See Table 15 for the sources of the experimental measurements.

coefficients at the freezing temperature (ϕ_{fr}), which are fitted directly by the model, has already been discussed in section 4, and the values used here are listed in the last column of Table 1. The method of Zeleznik (*5*) (see his section 2.4) is used for the incorporation of freezing point data for the tetrahydrate. This relies on the fact that the temperature/composition relationship is such that, over a large temperature range, two concentrations of aqueous H_2SO_4 are in equilibrium with the solid phase at any given value of T. For each measured freezing temperature, a corresponding concentration on the opposite part of the curve is estimated by interpolation. An activity product $a(H^+)^2 a(SO_4^{2-}) a_1^4$ is defined for the solid phase $H_2SO_4 \cdot 4H_2O$ (see also section 7). For the pairs of points, the difference

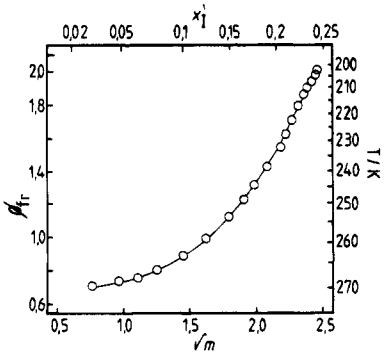

Figure 16. Stoichiometric molal osmotic coefficient (ϕ_{fr}) of aqueous H_2SO_4 at the freezing point of the solution, calculated from freezing point depression data of Gable *et al.* (*44*). The temperature is indicated on the right scale. The solid line indicates the fitted model.

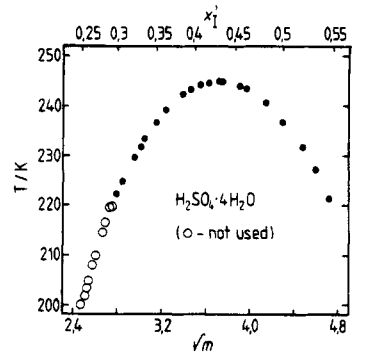

Figure 17. Freezing point curve for $H_2SO_4 \cdot 4H_2O$, data of Gable *et al.* (*44*). Temperatures for which there is saturation at only a single concentration (below about 220 K) were not used in the fit.

between the two calculated activity products (which must be 0) is fitted.

The data for the ice solid phase were given characteristic weights (w_c) one-eighth of those assigned to other osmotic coefficient data, to reflect the lower precision and the uncertainties involved in the calculation of ϕ_{fr}. For the solid phase $H_2SO_4 \cdot 4H_2O$, the data were weighted such that the contribution to the overall sum of squared deviations was about 2%. Both sets of measurements are shown in Figures 16 and 17.

Literature Cited

(1) Staples, B. R.; Wobbeking, T. F. NBSIR 81-2276; U.S. Government Printing Office: Washington, DC, 1981.
(2) Staples, B. R. *J. Phys. Chem. Ref. Data* **1981**, *10*, 779.
(3) Rard, J. A.; Habenschuss, A.; Spedding, F. H. *J. Chem. Eng. Data* **1976**, *21*, 374.
(4) Bolsaitis, P.; Elliott, J. F. *J. Chem. Eng. Data* **1990**, *35*, 69.
(5) Zeleznik, F. J. *J. Phys. Chem. Ref. Data* **1991**, *20*, 1157.
(6) Clegg, S. L.; Rard, J. A.; Pitzer, K. S. *J. Chem. Soc., Faraday Trans.* **1994**, *90*, 1875.
(7) Pilinis, C.; Seinfeld, J. H.; Seigneur, C. *Atmos. Environ.* **1987**, *21*, 943.
(8) Clarke, A. D.; Ahlquist, N. C.; Covert, D. S. *J. Geophys. Res.* **1987**, *92*, 4179.
(9) Spann, J. F.; Richardson, C. B. *Atmos. Environ.* **1985**, *19*, 819.
(10) Zhang, R. Y.; Wooldridge, P. J.; Molina, M. J. *J. Phys. Chem.* **1993**, *97*, 8541.
(11) Luo, B. P.; Clegg, S. L.; Peter, Th.; Muller, R.; Crutzen, P. J. *Geophys. Res. Lett.* **1994**, *21*, 49.
(12) Molina, M. J.; Zhang, R. Y.; Wooldridge, P. J.; McMahon, J. R.; Kim, J. E.; Chang, H. Y. *Science* **1993**, *261*, 1418.
(13) Pitzer, K. S.; Simonson, J. M. *J. Phys. Chem.* **1986**, *90*, 3005.
(14) Clegg, S. L.; Pitzer, K. S.; Brimblecombe, P. *J. Phys. Chem.* **1992**, *96*, 9470; *98*, 1368.
(15) Robinson, R. A.; Stokes, R. H. *Electrolyte Solutions*, 2nd ed. (revised); Butterworth: London, 1965.
(16) Young, T. F.; Maranville, L. F.; Smith, H. M. In *The Structure of Electrolytic Solutions*; Hamer, W. J., Ed.; Wiley: New York, 1959; pp 35–63.
(17) Archer, D. G.; Wang, P. *J. Phys. Chem. Ref. Data* **1990**, *19*, 371.
(18) Pitzer, K. S. *J. Solution Chem.* **1975**, *4*, 249.
(19) Pitzer, K. S. In *Activity Coefficients in Electrolyte Solutions*, 2nd ed.; Pitzer, K. S., Ed.; CRC Press: Boca Raton, FL, 1991; pp 75–153.
(20) Press, W. H.; Flannery, B. P.; Teukolsky, S. A.; Vetterling, W. T. *Numerical Recipes*; Cambridge University Press: Cambridge, 1986.
(21) Hamer, W. J. In *The Structure of Electrolytic Solutions*; Hamer, W. J., Ed.; John Wiley and Sons: New York, 1959; pp 236–252.
(22) Covington, A. K.; Dobson, J. V.; Lord Wynne-Jones. *Trans. Faraday Soc.* **1965**, *61*, 2057.
(23) Evans, C. E.; Monk, C. B. *Trans. Faraday Soc.* **1971**, *67*, 2652.
(24) Young, T. F.; Irish, D. E. *Annu. Rev. Phys. Chem.* **1962**, *13*, 435.
(25) Cabani, S.; Gianni, P. *Anal. Chem.* **1972**, *44*, 253.
(26) Dickson, A. G.; Wesolowski, D. J.; Palmer, D. A.; Mesmer, R. E. *J. Phys. Chem.* **1990**, *94*, 7978.
(27) Pitzer, K. S.; Roy, R. N.; Silvester, L. F. *J. Am. Chem. Soc.* **1977**, *99*, 4930.
(28) Mussini, P. R.; Longhi, P.; Mussini, T.; Rondinini, S. *J. Chem. Thermodyn.* **1989**, *21*, 625.
(29) Hovey, J. K.; Hepler, L. G. *J. Chem. Soc., Faraday Trans.* **1990**, *86*, 2831.
(30) Speedy, R. J. *J. Phys. Chem.* **1987**, *91*, 3354.
(31) Young, T. F. *Chem. Rev.* **1933**, *13*, 103.
(32) Klotz, I. M.; Rosenberg, R. M. *Chemical Thermodynamics, Basic Theory and Methods*, 3rd ed.; Benjamin/Cummings: Menlo Park, CA, 1972.
(33) Zhang, R. Y.; Wooldridge, P. J.; Abbatt, J. P. D.; Molina, M. J. *J. Phys. Chem.* **1993**, *97*, 7351.
(34) Hill, P. G. *J. Phys. Chem. Ref. Data* **1990**, *19*, 1223.
(35) McDonald, J. E. *J. Geophys. Res.* **1965**, *70*, 1553.
(36) Bichowsky, F. R.; Rossini, F. D. *The Thermochemistry of the Chemical Substances*; Reinhold Publishing: New York, 1936.
(37) Timmermans, J. *The Physico-Chemical Constants of Binary Systems in Concentrated Solutions*; Interscience: New York, 1960; Vol. 4.
(38) Staples, B. R.; Garvin, D.; Smith-Magowan, D.; Jobe, T. L.; Crenca, J.; Jackson, C. R.; Wobbeking, T. F.; Joseph, R.; Brier, A.; Schumm, R. H.; Goldberg, R. N. NBS Special Publ. 718; U.S. Government Printing Office: Washington, DC, 1986.
(39) Giauque, W. F.; Hornung, E. W.; Kunzler, J. E.; Rubin, T. R. *J. Am. Chem. Soc.* **1960**, *82*, 62.
(40) Rard, J. A. *J. Chem. Eng. Data* **1983**, *28*, 384.
(41) Rard, J. A.; Platford, R. F. In *Activity Coefficients in Electrolyte Solutions*, 2nd ed.; Pitzer, K. S., Ed.; CRC Press: Boca Raton, FL, 1991; pp 209–277.
(42) Gmitro, J. I.; Vermeulen, T. *AIChE J.* **1964**, *10*, 740.
(43) Numerical Algorithms Group. *FORTRAN Library Mk. 15*; NAG: Oxford, 1991.
(44) Gable, C. M.; Betz, H. F.; Maron, S. H. *J. Am. Chem. Soc.* **1950**, *72*, 1445.
(45) Kunzler, J. E.; Giauque, W. F. *J. Am. Chem. Soc.* **1952**, *74*, 5271.
(46) Weast, R. C., Ed. *CRC Handbook of Chemistry and Physics*, 64th ed.; CRC Press: Boca Raton, FL, 1983.
(47) Greenwood, N. N.; Wichers, E.; Peiser, H. S.; Gueron, J.; Cameron, A. E.; Fujiwara, S.; Roth, E.; Spaepen, J.; Thode, H. G.; Wapstra, A. H.; Flerov, G. N.; Svec, H. J. *Pure Appl. Chem.* **1970**, *21*, 91.
(48) Goldberg, R. N.; Weir, R. D. *Pure Appl. Chem.* **1992**, *64*, 1545.
(49) Archer, D. G. *J. Phys. Chem. Ref. Data* **1992**, *21*, 793.
(50) Hamer, W. J.; Wu, Y. *J. Phys. Chem. Ref. Data* **1972**, *1*, 1047.
(51) Shankman, S.; Gordon, A. R. *J. Am. Chem. Soc.* **1939**, *61*, 2370.
(52) Jones, F. R. *J. Appl. Chem., Suppl. Issue 2* **1951**, *1*, s144.
(53) Grollman, A.; Frazer, J. C. W. *J. Am. Chem. Soc.* **1925**, *47*, 712.
(54) Hepburn, J. R. I. *Proc. Phys. Soc. London* **1928**, *40*, 249.
(55) Nair, V. S. K.; Nancollas, G. H. *J. Chem. Soc.* **1958**, 4144.
(56) Davies, C. W.; Jones, H. W.; Monk, C. B. *Trans. Faraday Soc.* **1952**, *48*, 921.
(57) Hamer, W. J. *J. Am. Chem. Soc.* **1935**, *57*, 9.
(58) Harned, H. S.; Hamer, W. J. *J. Am. Chem. Soc.* **1935**, *57*, 27.
(59) Covington, A. K.; Dobson, J. V.; Lord Wynne-Jones. *Trans. Faraday Soc.* **1965**, *61*, 2050.
(60) Beck, W. H.; Singh, K. P.; Wynne-Jones, W. F. K. *Trans. Faraday Soc.* **1959**, *55*, 331.
(61) Beck, W. H.; Dobson, J. V.; Wynne-Jones, W. F. K. *Trans. Faraday Soc.* **1960**, *56*, 1172.
(62) Craig, D. N.; Vinal, G. W.; Vinal, F. E. *J. Res. Natl. Bur. Stand. (U.S.)* **1936**, *17*, 709.
(63) Kunzler, J. E.; Giauque, W. F. *J. Am. Chem. Soc.* **1952**, *74*, 3472.
(64) Wu, Y. C.; Young, T. F. *J. Res. Natl. Bur. Stand. (U.S.)* **1980**, *85*, 11.
(65) Groenier, W. L. Ph.D. Thesis, University of Chicago, Chicago, 1933.
(66) Lange, E.; Monheim, J.; Robinson, A. L. *J. Am. Chem. Soc.* **1933**, *55*, 4733.
(67) Abel, E. *J. Phys. Chem.* **1946**, *50*, 260.
(68) Biron, E. *Russ. Fiz.-Khim. Obsh.* **1899**, *31*, 171.
(69) Socolik, A. S. *Z. Phys. Chem.* **1932**, *158A*, 305.
(70) Craig, D. N.; Vinal, G. W. *J. Res. Natl. Bur. Stand. (U.S.)* **1940**, *24*, 475.

(71) Randall, M.; Taylor, M. D. *J. Phys. Chem.* **1941**, *45*, 959.
(72) Gardner, W. L.; Jekel, E. C.; Cobble, J. W. *J. Phys. Chem.* **1969**, *73*, 2017.
(73) Hood, G. C.; Reilly, C. A. *J. Chem. Phys.* **1957**, *27*, 1126.
(74) Stokes, R. H. *J. Am. Chem. Soc.* **1945**, *67*, 1689.
(75) Robinson, R. A. *Trans. R. Soc. N.Z.* **1945**, *75*, 203.
(76) Sheffer, H.; Janis, A. A.; Ferguson, J. B. *Can. J. Res.* **1939**, *17B*, 336.
(77) Scatchard, G.; Hamer, W. J.; Wood, S. E. *J. Am. Chem. Soc.* **1938**, *60*, 3061.
(78) Robinson, R. A. *Trans. Faraday Soc.* **1939**, *35*, 1229.
(79) Hornung, E. W.; Giauque, W. F. *J. Am. Chem. Soc.* **1955**, *77*, 2744.
(80) Collins, E. M. *J. Phys. Chem.* **1933**, *37*, 1191.
(81) Rard, J. A.; Miller, D. G. *J. Chem. Eng. Data* **1981**, *26*, 38.
(82) Rard, J. A.; Miller, D. G. *J. Chem. Eng. Data* **1981**, *26*, 33.
(83) Platford, R. F. *J. Chem. Eng. Data* **1973**, *18*, 215.
(84) Tarasenkov, D. N. *J. Appl. Chem. USSR* **1955**, *28*, 1053.
(85) Glueckauf, E.; Kitt, G. P. *Trans. Faraday Soc.* **1956**, *52*, 1074.
(86) Lewis, G. N.; Lacey, W. N. *J. Am. Chem. Soc.* **1914**, *36*, 804.
(87) MacDougall, F. H.; Blumer, D. R. *J. Am. Chem. Soc.* **1933**, *55*, 2236.
(88) Randall, M.; Cushman, O. E. *J. Am. Chem. Soc.* **1918**, *40*, 393.
(89) Schwabe, K.; Ferse, E. *Ber. Bunsen-Ges. Phys. Chem.* **1965**, *69*, 383.
(90) Trimble, H. M.; Ebert, P. F. *J. Am. Chem. Soc.* **1933**, *55*, 958.
(91) Tartar, H. V.; Newschwander, W. W.; Ness, A. T. *J. Am. Chem. Soc.* **1941**, *63*, 28.
(92) Vosburgh, W. C.; Craig, D. N. *J. Am. Chem. Soc.* **1929**, *51*, 2009.
(93) Shrawder, J.; Cowperthwaite, I. A. *J. Am. Chem. Soc.* **1934**, *56*, 2340.
(94) Rossini, F. D.; Gucker, F. T.; Johnston, H. L.; Pauling, L.; Vinal, G. W. *J. Am. Chem. Soc.* **1952**, *74*, 2699.
(95) Milioto, S.; Simonson, J. M., 48th Annual Calorimetry Conference, Durham, NC, 1993; Program Abstracts.
(96) Söhnel, O.; Novotný, P. *Densities of Aqueous Solutions of Inorganic Substances*; Elsevier: Amsterdam, 1985.
(97) Larson, J. W.; Zeeb, K. G.; Hepler, L. G. *Can. J. Chem.* **1982**, *60*, 2141.
(98) Hornung, E. W.; Brackett, T. E.; Giauque, W. F. *J. Am. Chem. Soc.* **1956**, *78*, 5747.
(99) Rubin, T. R.; Giauque, W. F. *J. Am. Chem. Soc.* **1952**, *74*, 800.
(100) Kunzler, J. E.; Giauque, W. F. *J. Am. Chem. Soc.* **1952**, *74*, 797.
(101) Hornung, E. W.; Giauque, W. F. *J. Am. Chem. Soc.* **1955**, *77*, 2983.
(102) Edward, J. T.; Wang, I. C. *Can. J. Chem.* **1965**, *43*, 2867.
(103) Turner, D. J. *J. Chem. Soc., Faraday Trans. 1* **1974**, *70*, 1346.
(104) Sherrill, M. S.; Noyes, A. A. *J. Am. Chem. Soc.* **1926**, *48*, 1861.
(105) Lindstrom, R. E.; Wirth, H. E. *J. Phys. Chem.* **1969**, *73*, 218.
(106) Chen, H.; Irish, D. E. *J. Phys. Chem.* **1971**, *75*, 2672.
(107) Kerker, M. *J. Am. Chem. Soc.* **1957**, *79*, 3664.
(108) Giauque, W. F.; Stout, J. W. *J. Am. Chem. Soc.* **1936**, *58*, 1144.
(109) Stull, D. R.; Prophet, H. *JANAF Thermochemical Tables*, NSRDS-NBS 37; U.S. Government Printing Office: Washington, DC, 1971.

Received for review September 7, 1993. Revised March 31, 1994. Accepted August 8, 1994.[⊗]

JE930179B

[⊗] Abstract published in *Advance ACS Abstracts,* November 15, 1994.